

UNIVERSITY OF LISBON  
FACULTY OF SCIENCES  
DEPARTMENT OF ANIMAL BIOLOGY



**UNIVERSIDADE  
DE LISBOA**

**NEUROPROTECTIVE PEPTIDES IN ALZHEIMER'S DISEASE:  
STRUCTURAL CHARACTERIZATION AND AFFINITY OF B-  
AMYLOID AND HUMAN CYSTATIN C PEPTIDES  
INTERACTIONS**

**Ana Almeida**

MASTER IN HUMAN BIOLOGY AND ENVIRONMENT

2009

UNIVERSITY OF LISBON  
FACULTY OF SCIENCES  
DEPARTMENT OF ANIMAL BIOLOGY



**UNIVERSIDADE  
DE LISBOA**

**NEUROPROTECTIVE PEPTIDES IN ALZHEIMER'S DISEASE:  
STRUCTURAL CHARACTERIZATION AND AFFINITY OF B-  
AMYLOID AND HUMAN CYSTATIN C PEPTIDES  
INTERACTIONS**

**Ana Almeida**

Intern Coordinator: Prof. Dra. Deodália Dias

Extern Coordinator Prof. Dr Dr h.c. Michael Przybylski

MASTER IN HUMAN BIOLOGY AND ENVIRONMENT

2009

*For my wonderful parents Maria and Julio Almeida.*

*“Do not follow where the path may lead. Go, instead, where there is no path and leave a trial.”*

*Anonymous*

*“Learn from yesterday, live for today, hope for tomorrow. The important thing is to not stop questioning. Curiosity has its own reason for existing.”*

*Albert Einstein*

The present work was carried out in the time from July 2008 to July 2009 in the Laboratory of Analytical Chemistry and Biopolymer Structure Analyses, Department of Chemistry of the University of Konstanz, under the supervision of Prof. Dr. Dr. h. c. Michael Przybylski.

I would like to thank to:

Prof. Dr. Dr. h. c. Michael Przybylski for the opportunity to work in his group, for the interesting topic and discussions concerning my work and for his entire support.

All members of the group for the nice and inspiring atmosphere, especially to Gabriela Paraschiv, Claudia Cozma, Mihaela Dragusanu, Marilena Manea, Camelia Vlad, Stefan Slamnoiu and Reinhold Weber for scientific discussions and all support that they gave to me in defining this work, as well as Paulina Czaplewska, from the University of Gdansk.

My family, for supporting and encouraging me during this time.

All my friends in Konstanz and Lisbon.

---

# TABLE OF CONTENTS

1. INTRODUCTION	1
1.1 Alzheimer's disease: Pathophysiological characteristics and potential therapeutical approaches	1
1.1.1 Biochemistry of Alzheimer's disease	1
1.1.2 Amyloid cascade hypothesis of Alzheimer's disease	4
1.2 Human cystatine c peptides in Alzheimer's disease	5
1.3 Methods and instrumentation of biopolymer	8
1.4 Introduction to affinity-mass spectrometry: Analytical methods for identification of ligand-binder interactions	11
1.5 Affinity interaction analysis using a surface acoustic wave biosensor system	14
1.6 Aims of the thesis	18
2. RESULTS AND DISCUSSION	19
2.1 Synthesis and structural characterization of $\beta$ -amyloid and hCC peptides	19
2.2 Mass spectrometric characterization of human cystatine c-amyloid $\beta$ epitope peptide complex	22
2.3 Affinity interaction hCC and amyloid $\beta$ -peptides system by SAW	23
2.4 SAW bioaffinity studies of amyloid- $\beta$ and hCC peptides	25
2.5 Determination of dissociation constant of amyloid $\beta$ and hCC peptides by SAW	29
2.6 Inhibition of amyloid $\beta$ -fibril formation by C-terminal hCC epitopes	34
2.7 Mass spectrometry	36
3. EXPERIMENTAL PART	40
3.1 Material and reagents	40
3.2 Solid phase peptide synthesis	40
3.3 High performance liquid chromatography	42
3.4 Gel electrophoresis	44
3.4.1 SDS-PAGE	44
3.4.2 Staining of the gels with Coomassie Brilliant Blue	45

---

3.5 Inhibition assay of amyloid $\beta$ -oligomerization by hCC peptides	46
3.6 Immunoanalytical methods	46
3.6.1 Enzyme Linked ImmunoSorbant assay (ELISA)	46
3.6.2 SAW Biosensor	47
3.6.3 ZipTip desalting and clean up procedure	49
3.6.4 ESI-Ion Trap mass spectrometer	50
3.7 Computer programs	51
3.7.1 GPMAW	51
4. SUMMARY	53
5. REFERENCES	56
6. APPENDIX	66
6.1 Appendix 1: Abbreviations	62
6.2 Appendix 2: Abbreviations for amino acids	63

# **1. INTRODUCTION**

## **1.1 Alzheimer's disease: Pathophysiological characteristics and potential therapeutical approaches**

Age-related impairments in cognition and memory have been known since ancient times, but the clinical-pathological features of the syndrome, now termed Alzheimer's disease (AD), were not documented in the literature until the first decade of last century (1906), when the German neurologist Alois Alzheimer reported the case of a middle-aged woman who developed memory deficits and progressive loss of cognition. AD is characterized by cognitive symptoms like memory loss, disorientation and confusion, problems with reasoning and thinking and by behavioral symptoms that include agitation, anxiety, depression, hallucination, insomnia and wandering.

It is established that AD is a progressive, degenerative disorder of the brain and the most common form of dementia among the elderly, affecting more than 20 million people worldwide. It is recognized as a major public health problem in developed nations and the third most expensive disease to treat in the U.S., costing society close to \$100 billion annually. There is currently no cure for AD and the exact causes of the disease are still unknown, but current research is beginning to allow a greater understanding of how this disease develops and potential therapeutic approaches to treat or prevent AD under investigation.

### **1.1.1 Biochemistry of Alzheimer's disease**

Microscopic examination of the AD brain reveals a number of characteristic histological lesions comprising intracellular neurofibrillary tangles (NFTs), extracellular amyloid plaques, congophilic angiopathy (CA) of the vessels, neuropil treads that lead to extensive neuronal loss, predominantly of the cholinergic neurons. Since the innervate



---

the hippocampus and cortex and are believed to be involved in information processing and storage, their loss is responsible for severe memory loss and behavioural and intellectual deterioration seen in AD.

Neurofibrillary tangles are neuronal cytoplasmic accumulations of paired helical filaments consisting of hyperphosphorylated *tau* protein, a neuron-specific phosphoprotein that is the major constituent of neuronal microtubules. The microtubules help transport nutrients and other important substances from one part of the nerve cell to another. In AD the *tau* protein is abnormal and the microtubule structures collapse. Intracellular protein accumulation is not specific for Alzheimer's disease alone, but has been shown in other degenerative disease.

The other neuropathological feature of AD is the accumulation and invariant deposition of extracellular beta-amyloid plaques (senile plaques) in the brain. Two major types of senile plaques have been identified: the classic (neuritic) and the diffuse senile plaques. The major component of either plaque type is the amyloid beta peptide ( $A\beta$ ), a 39-43 amino acid peptide derived from its precursor amyloid protein ( $\beta$ APP) by proteolytic processing. Whereas classic senile plaques consist of a central core of amyloid, made up of  $A\beta$  fibrils and surrounded by a halo of degenerating and dystrophic neuritis, the diffuse senile plaque contains non-fibrillar  $A\beta$  and contains neither an amyloid core nor neuritic changes (they are more abundant in AD brains than the classic senile plaques, but are also found in the brains of non-demented elderly).

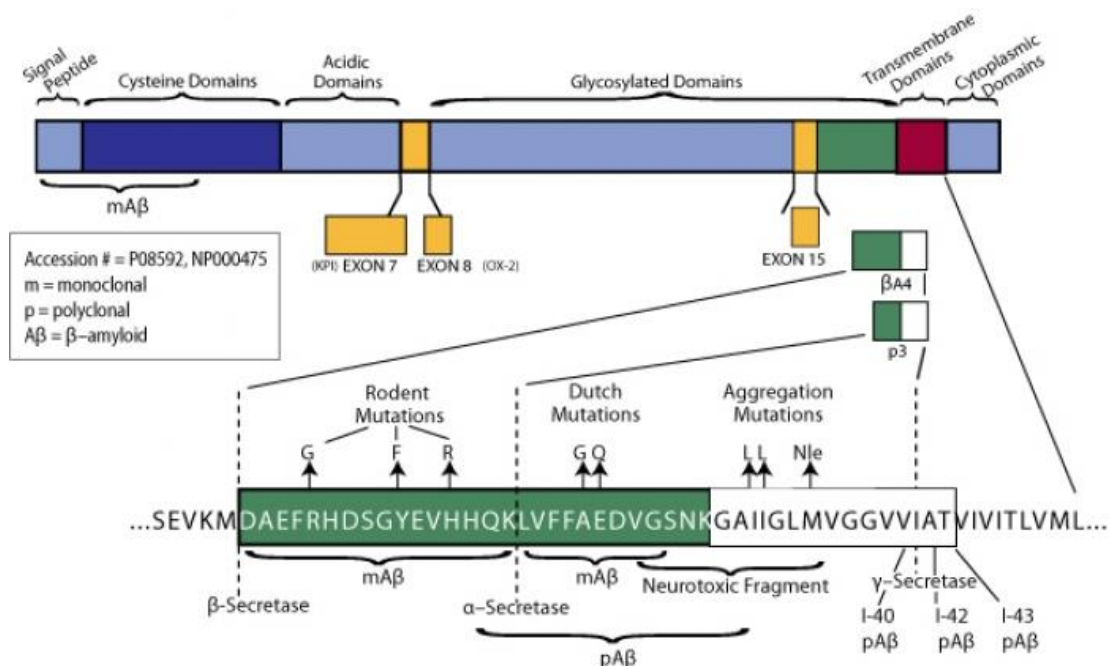


Figure 1: APP and Aβ protein schematic.

βAPP is a transmembrane glycoprotein with a single membrane spanning region, a large extracytoplasmic domain (ectodomain) and a small C-terminal intracytoplasmic part. It is expressed in the heart, kidneys, lungs, spleen and intestines, as well as in the brain. The most abundant isoforms in the brain are APP695, APP751 and APP770. APP695 is the shortest of the three isoforms and is produced mainly in neurons. APP 751, which contains Kunitz-protease inhibitor domain (KPI), and APP770, which contains both the KPI and an Ox<sup>2</sup> antigen domain, are found mostly in non-neuronal glial cells. All three isoforms share the same Aβ transmembrane and intracellular domains and are thus all potentially amyloidogenic.

The initial step of the metabolic pathway of APP involves the alfa-secretase enzyme that cleaves out APP within the Aβ sequence, allowing for the release of its transmembrane fragment. This metabolic pathway is not amyloidogenic because it precludes the formation of Aβ and leads to the release of APPα which appears to exert neuroprotective activity. Several reports suggested that mainly adamalysin proteinases such as ADAM 10 (a disintegrin and metalloprotease) or ADAM 17 (also known as

TACE, tumor necrosis factor converting enzyme) are involved in the constitutive and regulated alpha-secretory pathway of APP.

The alternative pathway of APP secretion results in the cleavage of APP at  $\beta$ - and  $\gamma$ -cleavage sites, liberating secreted APP (sAPP $\beta$ ) and A $\beta$  peptide. Recently, proteases that cleave APP at the  $\beta$ -site have been cloned and identified. They are named BACE 1 and 2 for beta-site cleaving enzyme and belong to the family of aspartyl-proteases.

$\gamma$ -Secretase is a hetero-oligomer containing at least four protein components, presenilins (PS-1/PS-2), nicastrin, APH-1 and PEN-2, in a high molecular mass complex of unknown stoichiometry.

A $\beta$  and A $\beta$ -like peptides have been found to be produced with strong N- and C-terminal heterogeneity. Under normal conditions, the most abundant species in the brain is the A $\beta$ 40; however much of the fibrillar A $\beta$  is composed of the longer, more fibrillogenic A $\beta$ 42. A $\beta$ 40 comprises 90-95% of the secreted A $\beta$  and it is the predominant species in cerebrospinal fluid (CSF). In contrast, less than 10% of secreted A $\beta$  is A $\beta$ 42. Originally, A $\beta$ 42 peptide was assumed to be released by a pathogenic event; it is now well established that A $\beta$ 42 is released from cells during normal cellular metabolism of the Alzheimer amyloid precursor protein. A $\beta$ 42 is the predominant species found in the plaques and is deposited initially to form insoluble amyloidogenic aggregates more rapidly than A $\beta$ 40.

### **1.1.2 Amyloid cascade hypothesis of Alzheimer's disease**

Several lines of evidence suggest that A $\beta$  plays a key role in the pathogenesis of AD. It was found that all patients with AD accumulate deposits of first A $\beta$ 42 and then also A $\beta$ 40 in regions of the brain important for memory, cognition and behavioural stability. A $\beta$ 42 diffuse plaques occur increasingly with age in neurologically normal individuals, strongly suggesting that A $\beta$ 42 accumulation precedes all other pathological features of AD.

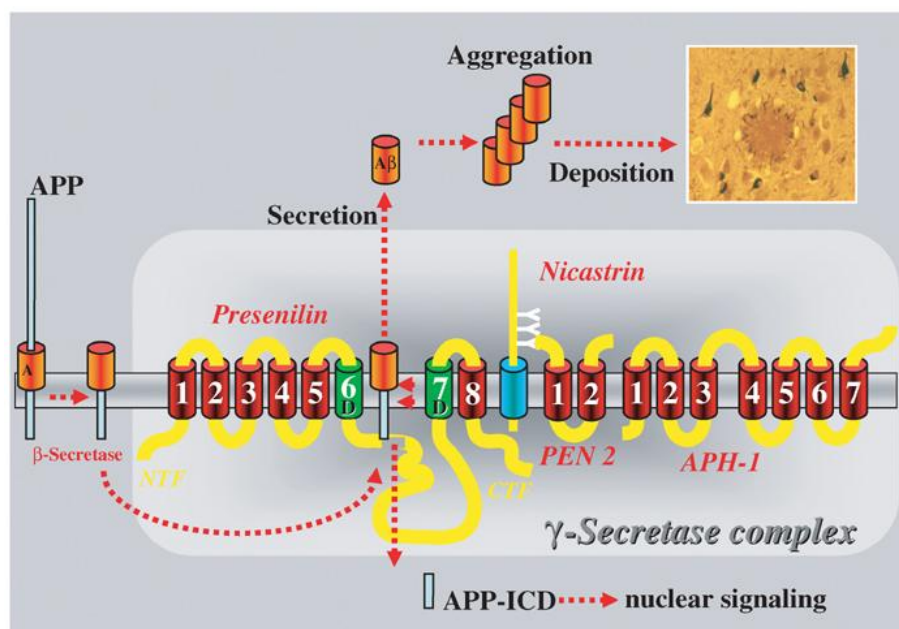


Figure 2: Generation of A $\beta$  from APP via proteolytic processing by  $\beta$ - and  $\gamma$ -secretase (for details, see text). A $\beta$  aggregates and finally precipitates in amyloid plaques. This event initiates the amyloid cascade resulting in additional intracellular aggregations of the tau protein, which then form tangles (the black structures surrounding the amyloid plaque).

## 1.2 Human cystatin c peptides in Alzheimer's disease

Alzheimer's disease (AD) and AD-related neurodegenerative disorders have become the predominant form of progressive cognitive failure in elderly humans, a development presently accelerating due to the significant increase in life expectancy in the last decades. Consequently, uncovering details of AD pathology has become of paramount importance. Major neuropathological features in AD brain are cortical atrophy, neuronal loss, regionspecific amyloid deposition, neuritic plaques and neurofibrillary tangles.[1,2] A major constituent of amyloid fibrils in brain of patients with AD and AD-related diseases, as well as in aged individuals without any neurological disorder is the  $\beta$ -amyloid polypeptide (A $\beta$ ). A $\beta$  arises from a large precursor, the amyloid precursor protein (APP); [3,4] it is produced by normal cells and detected as a circulating peptide in plasma and cerebrospinal fluid (CSF) of healthy humans.[5,6] Although the physiological role of APP is not well understood, specific missense mutations confer autosomal dominant inheritance of AD (FAD) and have pointed out pathogenic,

proteolytic processing mechanism(s).<sup>6</sup> The accumulation of A $\beta$ , a 39-42 amino acid proteolytic fragment of APP, in neuritic AD plaques is thought to be causative for disease progression.<sup>5,6</sup> The N-terminal sequence of A $\beta$ (1-42) is part of the extracellular region of APP, while the major C-terminal A $\beta$  sequence is contained within the transmembrane domain.

Despite the lack of details on degradation pathways and mechanism(s) of formation of A $\beta$ -derived plaques, recent studies towards the development of immunisation methods for AD based on therapeutically active antibodies have yielded initial success in generating antibodies capable of disaggregating A $\beta$ -plaques and reversing the memory impairments in transgenic AD mice. Both active immunisation with pre-aggregated A $\beta$ (1-42) and administration of antibodies against A $\beta$  significantly attenuated plaque deposition and neuritic dystrophy.<sup>[7,8,9]</sup> Thus, active or passive immunization of AD patients may emerge as a therapeutic approach targeting the production, clearance, and aggregation of A $\beta$ .<sup>[10,11]</sup> The molecular antigen recognition of antibodies produced by immunisation with A $\beta$  has been identified using selective proteolytic excision (epitope-excision) of antigen-antibody complexes in combination with high resolution mass spectrometry <sup>[12]</sup> , providing a specific N-terminal epitope, A $\beta$ (4-10); the same epitope of plaque-specific antibodies has been identified in AD plaques, extracts from A $\beta$ -protofibrils, and synthetic A $\beta$ (1-42).<sup>[12,13]</sup> Recently, natural anti-A $\beta$ - antibodies (A $\beta$ -autoantibodies) have been identified in both blood and CSF of nonimmunized humans,<sup>[14]</sup> which specifically bind to human A $\beta$ (1-40) as well as to A $\beta$  in brain of transgenic mice and have been shown to reduce A $\beta$ -fibrillation and neurotoxicity.<sup>[15-17]</sup> A $\beta$ -autoantibodies have been also found in intravenous IgG preparations (IVIgG), and treatment of AD patients with IVIgG caused a reduction of A $\beta$  concentrations in CSF<sup>15</sup> and neuroprotective effect in inhibiting A $\beta$ -plaque deposition.<sup>[16-18]</sup> A specific carboxy-terminal A $\beta$ -epitope has been identified to be targeted by A $\beta$ -autoantibodies using epitope excision mass spectrometry (M. Przybylski et al., *Abstr. 7th Austral. Pept. Sympos.* **2007**; Cairns, Oct. 21-25; 32), in contrast to A $\beta$ -antibodies produced by active immunisation.<sup>[17,18]</sup>

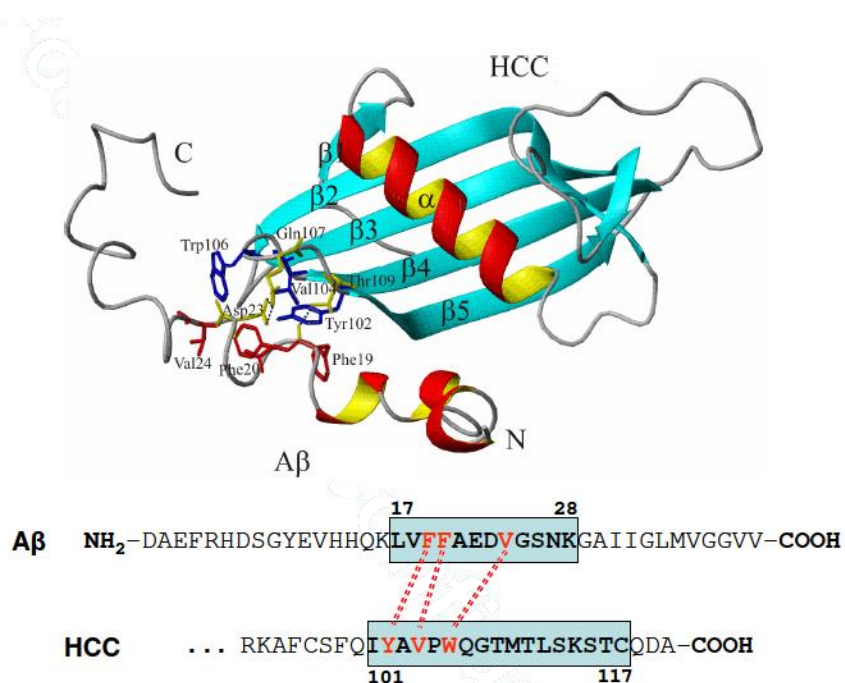


Figure 3: Interaction structure of the HCC-A $\beta$  complex revealed by molecular dynamics simulation. Hydrophobic interactions between HCC and A $\beta$ , Tyr-102, Val-104 and Trp-106 residues of HCC are colored in blue, Phe-19, Phe-20, Val-24 residues of A $\beta$  are colored in red. Hydrogen bonds between Gln-107 and Thr-109 residues of HCC and Asp-23 and Phe-19 of A $\beta$  are indicated by black dashed lines, respectively; amino acids and carbonyl groups (Phe-19) forming hydrogen bonds are colored in yellow.

Although amyloid plaques in brain of AD patients contain predominantly A $\beta$ -aggregates, immunohistochemical studies have shown the co-deposition of several other proteins, such as the protease inhibitor cystatin C, apolipoprotein E, clusterin, transthyretin and gelsolin.[19-22] In particular, the presence of human cystatin C (HCC) in amyloid deposits has found much interest,[23,24] and a wide spectrum of activities has been associated with HCC such as modulation of neuropeptide activation and neurite proliferation.[25,26] The 13 kDa protein HCC is the main cysteine protease inhibitor in mammalian body fluids[27,28] and has been found with high concentrations in CSF. While wild type cystatin C has no aggregation tendency, the naturally occurring mutant L68Q shows a high tendency to form amyloid fibrils, causing hereditary cerebral hemorrhage of the amyloidosis-Icelandic type.[20-23] The presence of HCC in A $\beta$ -plaques has been suggested to result from its binding to APP, or alternatively, HCC may bind to A $\beta$  prior to the secretion or following the deposition in brain.[23] Sastre et al. found that the association of HCC with A $\beta$  causes an inhibition of fibril formation, and

---

suggested an N-terminal A $\beta$ -sequence to be responsible for the interaction, with formation of a stoichiometric HCC-A $\beta$  complex.[25]

The recent results suggesting an important role of HCC in the processing and/or aggregation of A $\beta$  prompted our interest in the molecular characterization of the A $\beta$ -HCC interaction. Here we report the identification of the interacting epitopes of HCC and A $\beta$  using selective proteolytic excision of the HCC-A $\beta$  complex (epitope-excision) and mass spectrometry (MS).[18] The general analytical scheme of the epitope excision-MS approach is shown in Figure 1. Briefly, the immobilised ligand-binder (antigen-antibody) complex is subjected to specific, limited protease digestion followed by mass spectrometric analysis of the eluted affinity-bound epitope fragments. In the proteolytic step the ligand epitope is protected from digestion due to the shielding of the ligand-binder interaction, enabling subsequent specific dissociation and MS analysis of the bound epitope(s).<sup>18</sup> In a variation of this approach (“epitope-extraction”) the ligand is first subjected to proteolytic digestion and the mixture of peptide fragments presented to the immobilised binder. Using both MS approaches the A $\beta$ -epitope interacting with HCC was identified in a central, C-terminal A $\beta$  sequence interfering with the A $\beta$ -aggregation; an analogous proteolytic-MS approach with immobilised A $\beta$  provided the identification of a specific A $\beta$ -binding epitope at the C-terminus of HCC, HCC(101-117). Structures and affinities of both the A $\beta$  and HCC epitopes were characterised by ELISA, surface plasmon resonance (SPR), direct mass spectrometric analysis of HCC-A $\beta$ -epitope peptide complexes, and a structure model of the HCC-A $\beta$  complex obtained by molecular docking simulation. Furthermore, we show the functional activity of the identified synthetic HCC-epitope by analysis of its A $\beta$ -fibril inhibitory effect *in vitro*.

### 1.3 Methods and instrumentation of biopolymer

Mass spectrometry (MS) is today one of the major analytical methods. The information gained from the analyses of the intact or fragmented molecular ions can be used for the determination of structure and composition of pure substances or mixtures.

---

The general build-up of mass spectrometers suitable for biopolymer analyses can be summarized in a simple scheme of their basic components: ion source, mass analyzer and detector. The ion source is the place of ion formation from sample. The mass analyzer is responsible for the separation of ions according to their  $m/z$ . The ion signals from the detector, combined with other information from the ion source or the analyzer are transferred for processing to the computer that delivers the mass spectra.

The mass spectrometry became widespread in the biopolymer analyses only after the introduction of soft ionization methods, two most used today being matrix-assisted laser desorption ionization (MALDI) and electrospray ionization (ESI). Their importance has been also recognized by the awarding of the 2002 Nobel Prize for Chemistry to John B. Fenn [1] and Koichi Tanaka. [2]

Matrix-assisted laser desorption ionization (MALDI) [3] is a pulsed method in which the sample under vacuum or at atmospheric pressure [10] is irradiated with a laser (usually nitrogen laser, wavelength 337 nm, pulse duration 3-4 ns). The analyte is embedded in a so called matrix, which consists of crystals of small organic molecules that absorb strongly in the UV domain, close to the wavelength of the laser. Their role is to protect the analyte molecules from the high energy of the laser beam and allow them to remain intact during the ionization. They must also be acidic, in order to provide a proton source for the sample ionization. A typical used matrix is  $\alpha$ -cyano-4-hydroxycinnamic acid.



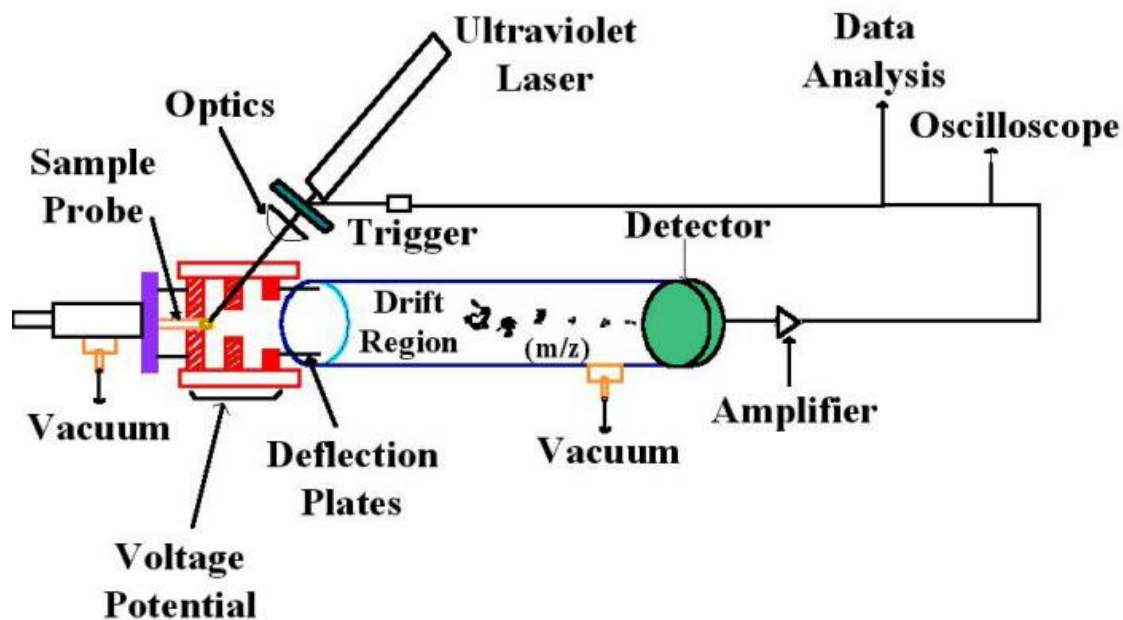


Figure 4: Matrix-assisted laser desorption ionization (MALDI).

Protonation and deprotonation is the main source of charging for biologically relevant ions in ESI. In fact, ions of proteins, peptides, oligonucleotides and other molecules with acid/base functionality are often found with several sites of protonation or deprotonation. The multi-charge ions are a typical characteristic for ESI, being also a major advantage. The multiple peaks from the ESI mass spectrum make the measurements more accurate. The large number of charges on the ions allows the mass spectrometers with limited  $m/z$  ranges to analyze high molecular weight molecules. Additionally to the ionization of very large molecules, ESI enables also the study of non-covalent bio-macromolecular complexes [14]. But the most important feature of ESI is the ease with which it can be coupled with other instruments. Particularly the association with HPLC systems is a very successful practice. Generally, ESI may be coupled with any kind of other instrument that delivers a continuous flow of solution to be analysed. However, ESI has also two notable deficiencies: i) the continuous spraying leads inevitably to waste of sample, as no mass spectrometer can continuously analyze ions; ii) the presence of salts in samples has a very negative impact on ESI formation. The second drawback can be overcome by first desalting the samples, this intermediate step being

rendered by different methods.

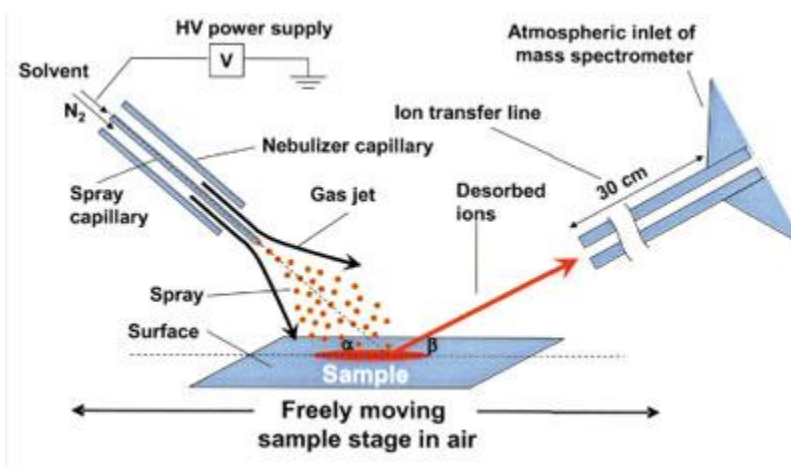


Figure 5: Electro spray ionization – principle of functioning: high positive potential is applied to the capillary (anode), causing positive ions in solution to drift towards the exit, where the liquid surface is distorted, forming a cone (“Taylor” cone); from the tip of the cone is emitted a spray of droplets with an excess of positive charge; gas phase ions are formed from charged droplets in a series of solvent evaporation steps.

## 1.4 Introduction to affinity-mass spectrometry: Analytical methods for identification of ligand-binder interactions

Affinity binding refers in general to those binding interactions between complex molecules of biological nature that are non-covalent and originating in a multitude of different physical interactions, like dipole interaction, hydrogen bond or hydrophobic interaction. Although every single physical interaction involved is weak, the affinity binding is their specificity. This is explained through a highly specific structure with a certain special location of different sites of interaction, required in order that all the types of non-covalent bindings are formed. This simplistic description is a lock-and key model [22,23] of the affinity interaction.

Affinity bindings are of crucial importance in most of the biochemical interactions involved in a living organism. Therefore their study has been always a source of precious information for understanding the mechanisms of different biological

processes. Particularly the investigation of the different diseases at molecular levels, in search of a new drug, has stimulated the study of affinity bindings. A major class of biomolecules, the proteins, owe their biological role to the capability to affinity bind other molecules like other proteins, peptides, carbohydrates, lipids, metal ions, antibody to its antigen is very interesting through the potential of the antibodies to become highly specific drugs against different types of targets. The antigen region of binding to the antibody is called antigenic determinant or epitope. The analogue region from antibody that binds to the epitope is called paratope. In the case that the antigen is a peptide or a protein, the epitope consists of one or more short sequences of amino acids. When there is only a single sequence, the epitope is said to be linear (continuous). In case of more sequences, the epitope is discontinuous.

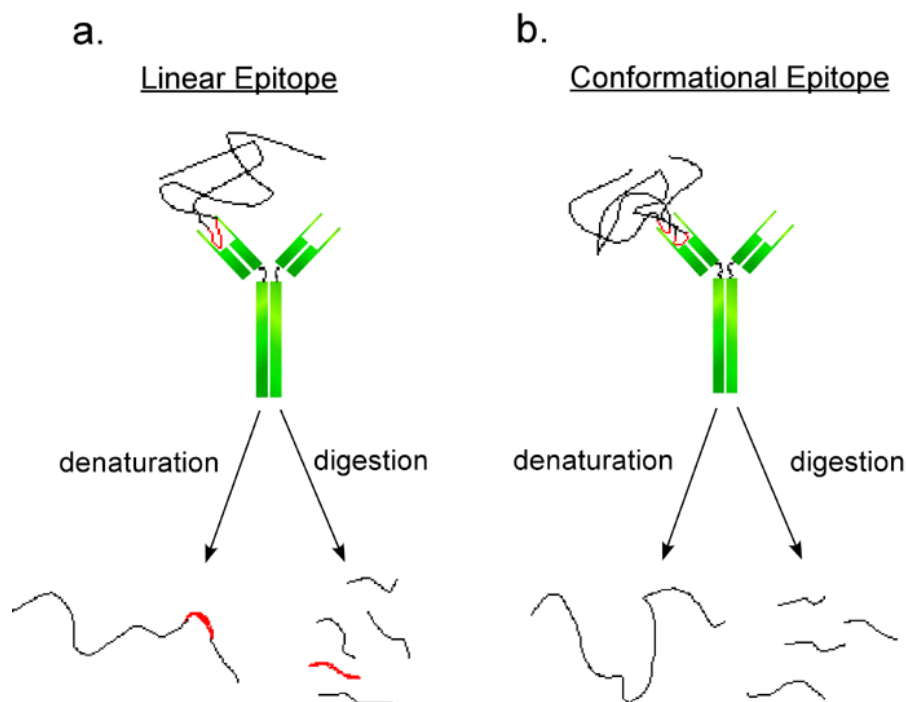


Figure 6: Schematic representation of the two types of epitopes found in proteins.

The identification and analysis of antigenic determinant is of crucial importance for the understanding of the binding between an antibody and an antigen, providing a starting point for the design of diagnostic tools or for the development of new vaccines [24,32].

There are several methods for the epitope identification, such as alanine-scanning

mutagenesis [25] or X-ray crystallography [26].

A molecular approach for identification of epitopes from peptide and protein antigens is the mass spectrometric epitope excision or extraction [27, 28]. Beside the capacity of investigation at the molecular level, this method offers many other advantages, such as time consume, sample quantity and purity, and employment of solution sample in the work flow.

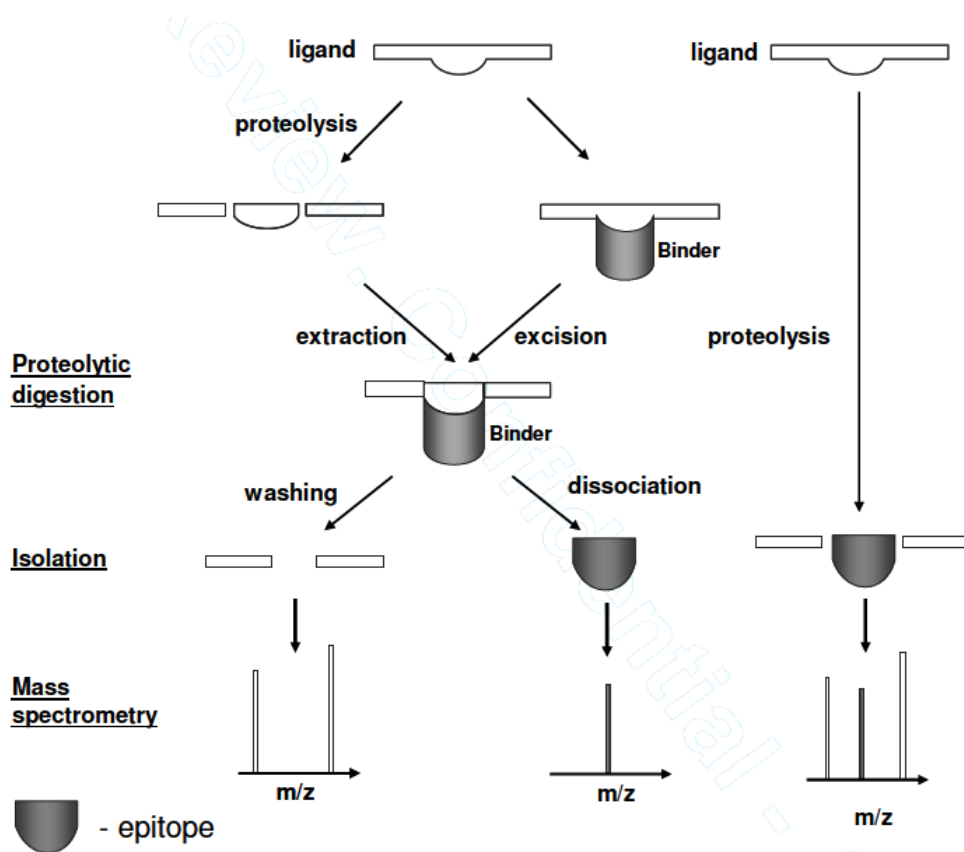


Figure 7: Schematic representation of mass spectrometric epitope excision and extraction procedures.

The principle of mass spectrometric epitope identification has been developed by our laboratory, and is based on the finding that the contact sides of the antigen are sterically protected by the antibody during the proteolyses [29]. In practice the antibody is covalently immobilized on a sepharose matrix and the antigen is allowed to bind to it. A specific protease digestion is then performed and the resulted fragments are eluted.

Bound to antibody remain only the epitope fragments, which are eluted under acidic conditions and then analyzed by mass spectrometry, for sequence identification (epitope excision). Alternatively, the digestion can be performed first and the mixture is added to the antibody micro-column. The epitope peptides can be separated through binding to the antibody, and then analyzed by mass spectrometry (epitope extraction). The discontinuous epitopes are more difficult to identify, their identification requires frequently a differential chemical modification [30, 62-65].

## 1.5 Affinity interaction analysis using a surface acoustic wave biosensor system

In the last three decades, the biosensors have been developed as a new and efficient tool of analytical chemistry. After Thévenot [33], “biosensors are chemical sensors in which the recognition system utilizes a biochemical mechanism”. Furthermore, he defines a chemical sensor as a combination of two elements: “a chemical (molecular) recognition system (receptor) and a psycho-chemical transducer”.

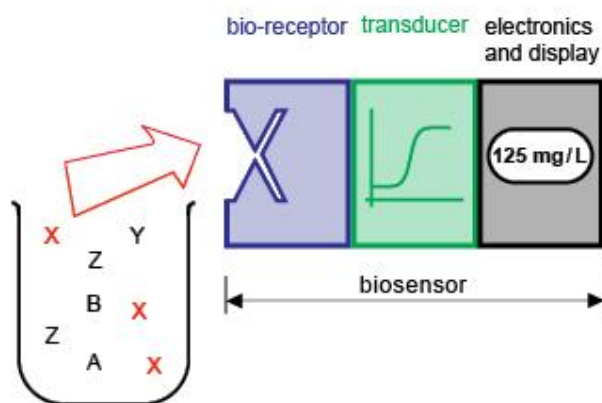


Figure 8: Schematic representation of the basic components of a biosensor: the biochemical sensitive element (bio-receptor) and the physical element responsible for signal generation (transducer).

Therefore, a biosensor has two major components: the biochemical sensitive element

and the physical element of signal generation. For the signal processing and results display a computer is usually used. Both major components are of various types and an exhaustive classification is not the purpose of this work. However, the physical elements of the biosensors are generally optical, electrochemical or electro-mechanical. Further, most of the electro-mechanical biosensors are based on the piezoelectric effect. The piezoelectric crystals can be made to vibrate at a specific frequency with the application of an electrical signal of a specific frequency. These oscillations are actually mechanical waves that travel through the bulk matter. Their frequency is dependent on the electrical frequency applied to the crystal as well as the crystal's mass. Therefore, when the mass increases due to binding of chemicals, the oscillation frequency changes and the resulting change can be measured electrically and be used to determine the additional mass of the crystal. This is the function principle of a quartz crystal microbalance (QCM) [34]. If the oscillation is confined in a thin layer on the surface of the crystal, one speaks of surface acoustic waves (SAW) [35, 36]. Different types of acoustic waves can be employed in a SAW device, but Love waves [35] offer particularly high sensitivities due to the confinement of the acoustic energy to the sensing surface (Figure 8). The Love wave are in fact shear horizontally polarized guided waves [36], being especially suited for sensing liquids [37]. The recently introduced K% biosensor system uses surface acoustic wave of Love type [38].

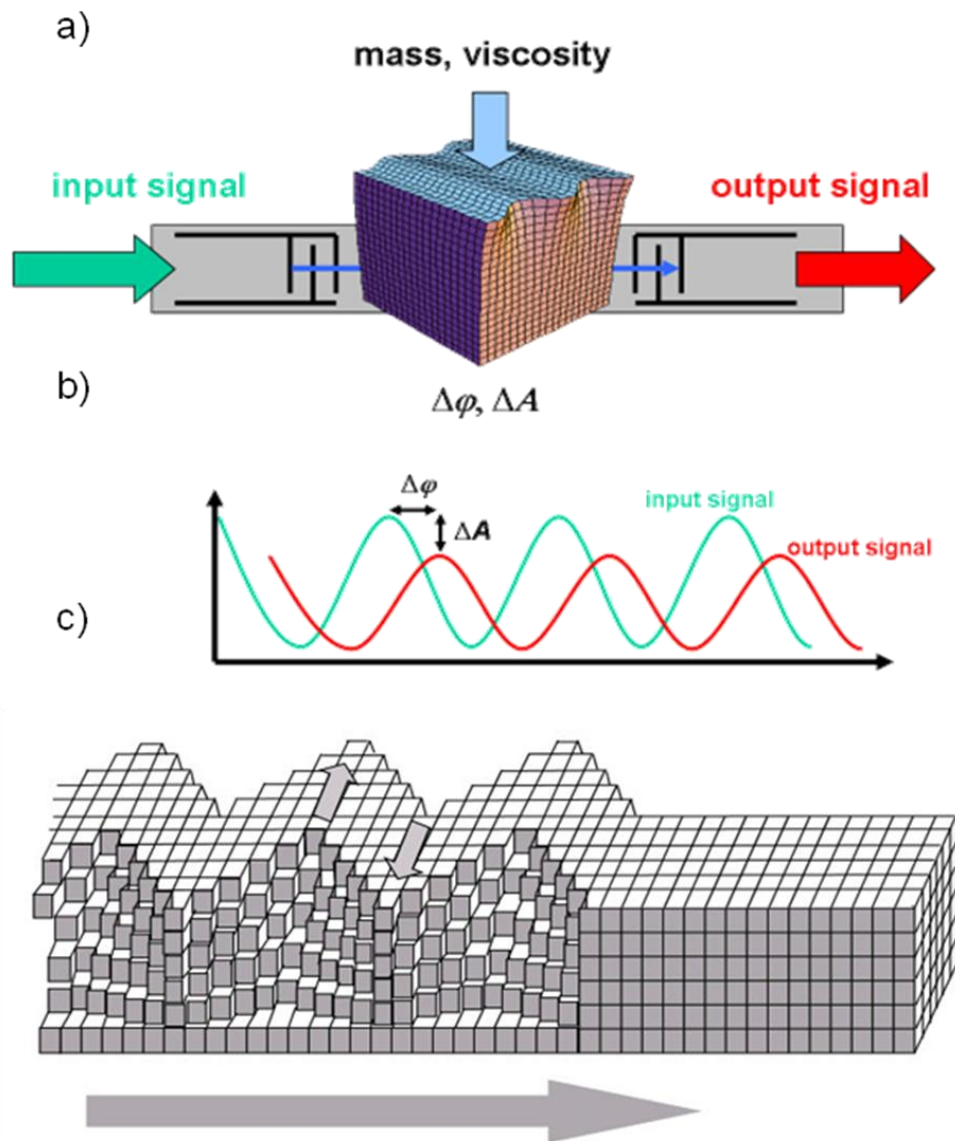


Figure 8: a) Functioning principle of the SAW sensor: an electrical signal is transformed in mechanical wave through piezoelectricity; the wave changes its amplitude and phase due to surface mass loading and liquid viscosity changes; the wave is then transformed back into electrical signal for processing; b) The input and output signals differ in phase and amplitude; mass loadings render phase shifts, while viscosity changes induce modification in both phase and shift; c) Love waves are horizontally polarized transversal waves.

The essential part of the instrument is the microstructured sensor-chip. This is a thin plate of quartz (the substrate) on which are deposited, by standard thin film deposition

and optical lithography processes, the contact pads for electronics and the interdigital transducers (IDTs) [38, 39]. The split finger design is used in order to reduce distortions from reflections. Over the IDTs there is deposited another layer of amorphous  $\text{SiO}_2$ , with a 4.5  $\mu\text{m}$  thickness. This is the “guiding layer” for the Love waves. On top of it the sensitive surface is covered with a thin (150 nm) film of Cr/Au alloy. On one single chip there are five sensor elements, which can be operated independently (Figure 9).

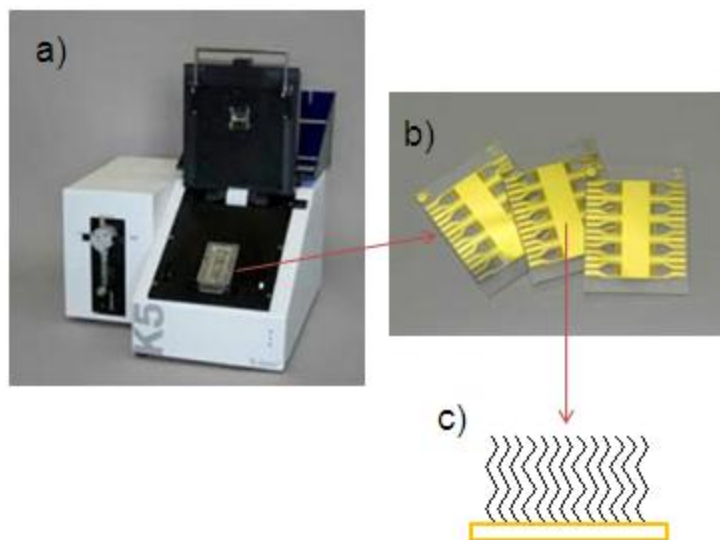


Figure 9: a) The K5 biosensor instrument, containing the electronics, the pump and the flow cell; b) the  $\text{SiO}_2$  chip, covered with a layer of gold. There are visible the sensing surfaces of the five channels, the contacts for electronics and the regions of interdigital transducers (IDTs). c) self assembled monolayer (SAM) formation on the gold sensitive surface, used as a linker for the covalent immobilization of different other molecules.

Further, the chemical components used in analysis are physically absorbed on the gold surface, or are fixed through a covalent bond (or a linker) to the gold layer. The most convenient method is the covalent binding to gold surface. This can be easily achieved with organic molecules containing free thiol groups employing the well known chemical affinity of sulphur for gold. With bifunctional molecules like 16-mercaptohexadecanoic acid different other molecules, capable of forming bonds with the carboxyl group (amines, alcohols, etc.), can be attached to the gold-surface. When employing 16-mercaptohexadecanoic acid, or other similar molecules, as a linker, an important



process occurs on the gold surface: the saturated carbon chains align themselves parallel one to another due to the hydrophobic interactions. This is the so called self assembled monolayer (SAM) [40-43]. The carboxyl groups of the 16-mercaptohexadecanoic acid can be activated using 1-ethyl-3-(3-(dimethylamino)propyl) carbodiimide hydrochloride (EDC) and N-hydroxy-succinimide (NHS) [44].

## 1.6 Aims of the thesis

The aims of the present thesis are summarized as follows:

1. *Synthesis and purification* of amyloid  $\beta$ -peptides including  $A\beta$  (1-40) and  $A\beta$  (17-28), as well as of hCC-peptides, more specifically hCC (101-117) and hCC (93-120).
2. *Characterization of affinity binding between  $A\beta$ -peptides and hCC-peptides by Surface Acoustic Wave (SAW) and ELISA* to compare the results obtained from both methods.
3. *Determination of the dissociation constant ( $k_d$ ) of  $A\beta$  peptides (using SAW biosensor).*
4. Study of the inhibition effect on the fibrillization process of  $A\beta$  observed in presence of hCC.

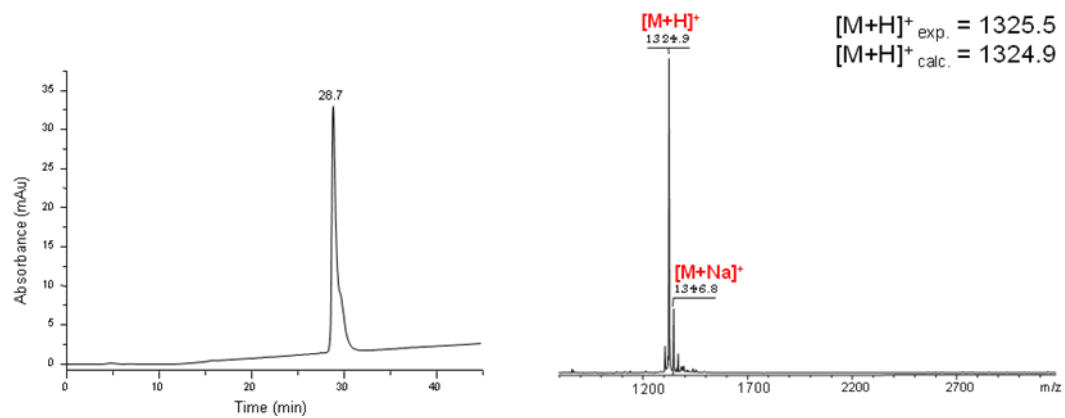
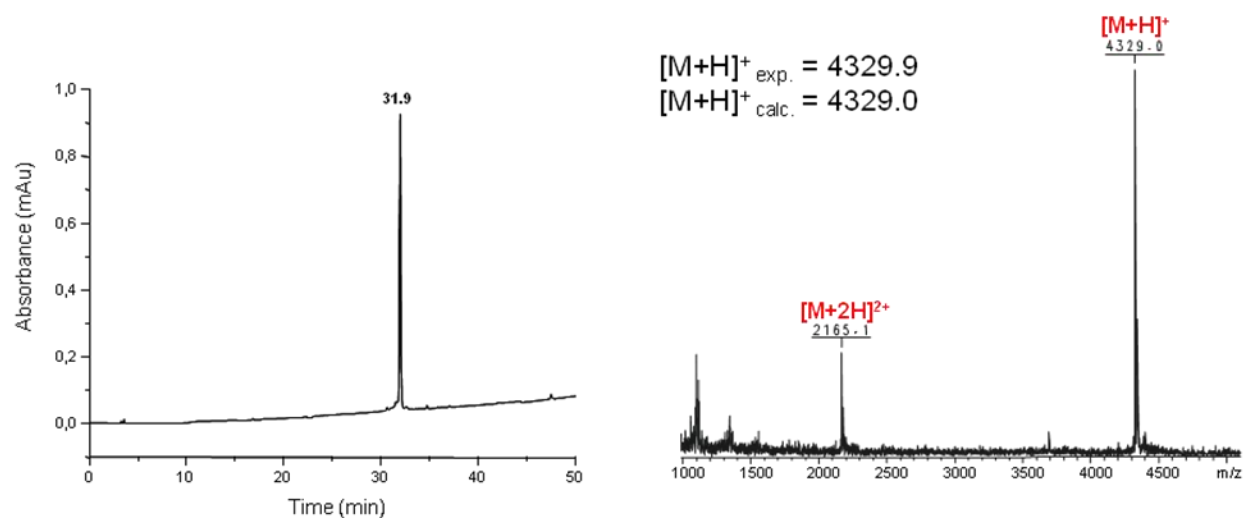
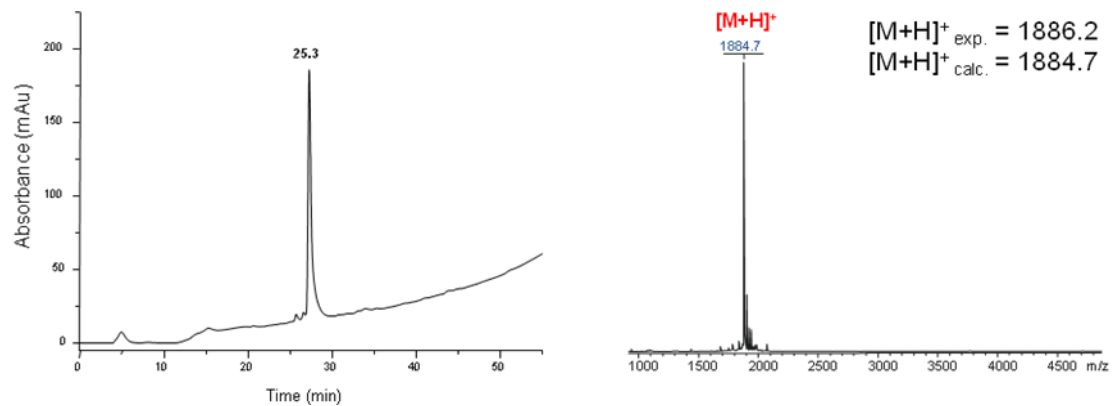
## 2. RESULTS AND DISCUSSION

### 2.1 Synthesis and structural characterization of beta-amyloid and HCC peptides

The synthesis of the peptides employed in this study was performed on a NovaSyn TGR resin according to fluorenylmethyloxycarbonyl (Fmoc)/tert-Butyl (tBu) chemistry. Double coupling was used to reach an almost complete formation of amide bond for each amino acid. The protocol of the synthesis consisted of removal of Fmoc group with 20% piperidine in dimethylformamide (DMF) for 8 minutes, coupling of PyBOP/NMM-activated amino acid for 30 minutes and washing. DMF was employed as a solvent for all the reactions and it was also used for all washing steps. After the desired sequence was completed, the cleavage of the peptide from the resin was carried out with TFA, triethylsilane and water for 3 hours at room temperature. The crude product was precipitated with t-butylmethylether, filtered, re-dissolved in 5% acetic acid and lyophilized. The crude product was purified by reversed phase high performance liquid chromatography (RP-HPLC) and analyzed by ESI ion trap MS. The amino acid sequences, the HPLC chromatograms and the mass spectra are shown in Table 1 and Figure 10.

Table 1: Chemical characteristics of A $\beta$ -peptides.

Peptide	Sequence	R <sub>t</sub> (min) <sup>a</sup>	Purity (%) <sup>b</sup>	[M+H] <sup>+</sup> <sub>Theo/Exp.</sub> <sup>c</sup>
A $\beta$ (1-40)	NH <sub>2</sub> -DAEFRHDSGYEVHHQKLVFFAE DVGSNKGAILMVGGVV-CONH <sub>2</sub>	31.9	94	4329.9 / 4329.0
A $\beta$ (17-28)	NH <sub>2</sub> -LVFFAEDVGSNK-CONH <sub>2</sub>	28.7	90	1325.5 / 1324.9
HCC (101-117)	NH <sub>2</sub> -IYAVPWQGTMTLSKSTC-CONH <sub>2</sub>	25.3	96	1886.2 / 1884.7
HCC (93-120)	NH <sub>2</sub> -RKAFCSFQIYAVPWQGTMTLSKS TCQDA-CONH <sub>2</sub>	31.9	95	3168.7 / 3168.2

**a.****b.****c.**

d.

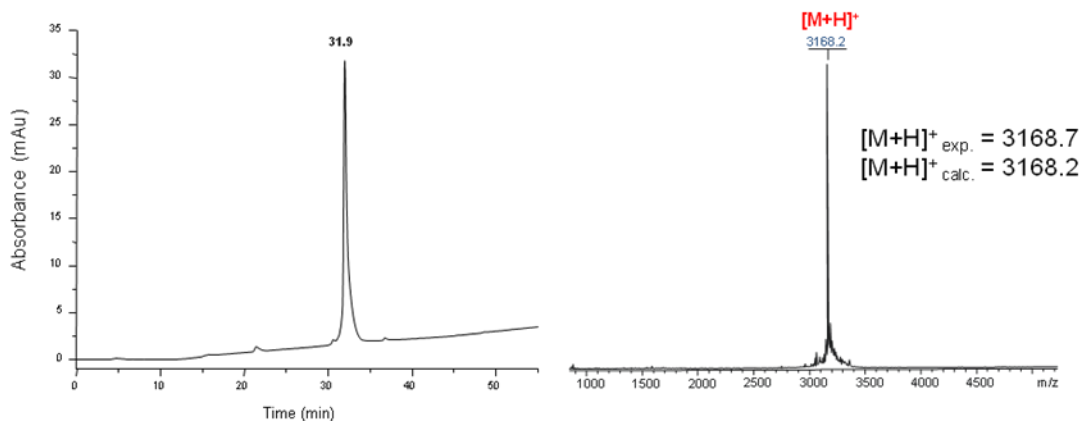


Figure 10: HPLC profile and the ESI ion trap mass spectrum of: **a.** A $\beta$  (17-28), **b.** A $\beta$  (1-40), **c.** hCC (101-117), **d.** hCC (93-120)

The investigation of the brain tissue from patients with Alzheimer's disease revealed the accumulation of A $\beta$  peptides.

The protease inhibitor human cystatin C (HCC) co-associates with  $\beta$ -amyloid (A $\beta$ ) in A $\beta$ -fibrils in brain of Alzheimer's disease patients by a specific interaction, the molecular basis of which has been elucidated in the present study. The binding epitopes and interaction structure of HCC and A $\beta$  in the stoichiometric A $\beta$ -HCC complex have been identified using a combination of selective proteolytic excision and high resolution mass spectrometry; they encompass a central sequence of A $\beta$  that inhibits fibril formation, and is consistent with the structure of the A $\beta$ -HCC complex obtained by molecular docking simulation. The molecular characterisation of the A $\beta$ -HCC interaction provides a basis to derive new neuroprotective AD and HCC amyloidosis therapeutic lead structures and AD diagnostics.

To proceed to the interaction studies, the synthesis of both peptides was necessary. A $\beta$  (17-28) comprehends the epitope of the larger peptide (A $\beta$ (1-40)) and theoretically an higher affinity, but the last one is one of the most common in the AD patients brains. In this way. In hCC case, the epitope (hcc(101-117)) and the larger peptide are of interested to see which one will interact more with the A $\beta$  peptides.

## 2.2 Mass spectrometric characterization of the HCC-A $\beta$ epitope peptide complex.

Further evidence for the specific interaction of the HCC- and A $\beta$ - epitopes was obtained by direct high resolution ESI- mass spectrometry of the complexes of HCC- and A $\beta$ - peptides. The nano ESI-FTICR mass spectrum of the peptide complex between the HCC(101-117) and the A $\beta$ (17-28) epitopes is shown in Figure 11. The specific formation of a stoichiometric complex between the two minimal epitope peptides is ascertained by the triply and quadruply charged molecular ions (M+3H)<sup>3+</sup> (m/z 1070,1408) and (M+4H)<sup>4+</sup> of the complex which were determined with a relative mass accuracy of approximately 5 ppm. Likewise, the complex between HCC(93-120) and A $\beta$ (17-28) yielded molecular ions (M+3H)<sup>3+</sup> (m/z 1497,6012) and (M+4H)<sup>4+</sup> (m/z 1123,4403) ( $\Delta$ m 6.5 ppm; not shown). Thus, the ESI- MS analysis of the peptide complex ascertained the specific interaction of the C-terminal HCC epitope with the A $\beta$  epitope located in the middle- to C- terminal domain.

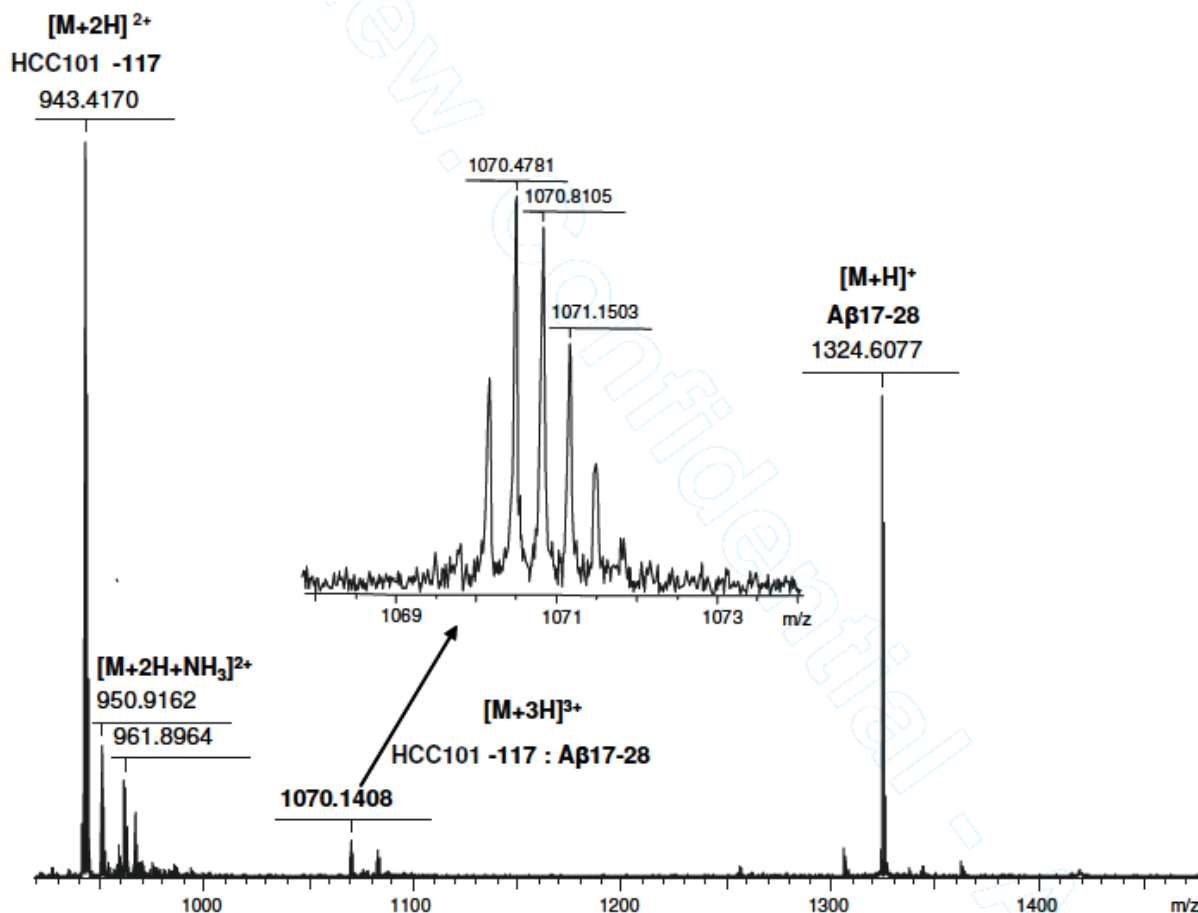


Figure 11: Nano ESI-FTICR mass spectrum of the peptide complex between the HCC(101-117) and the A $\beta$ (17-28) epitopes.

### 2.3 Affinity interaction hCC and A $\beta$ -peptides system by ELISA

The affinities interactions between the hCC-peptides and A $\beta$ -peptides were investigated by ELISA.

The Enzyme-Linked ImmunoSorbent Assay (ELISA) experiment was performed by coating the 96-well microtiter plate with 12 serial dilutions of peptides. The unspecific binding sites were blocked with bovine serum albumin (BSA) before adding the specific antibody with a dilution 1:1000. The systems investigated were .... For the detection was used anti-mouse antibody conjugated with horseradish peroxydase (HRP), diluted

1:5000.

In Figure 12 the optical density (OD) at  $\lambda$  450 nm is plotted versus antigen concentration.

The specificities and affinities of the epitope interactions were analysed by ELISA of the HCC and A $\beta$  peptides in an analogous manner as employed for antibody binding to an antigen-coated plate. A suitable ELISA approach for the A $\beta$ -HCC complex was developed to determine the affinities of A $\beta$  peptides to HCC, by absorption of HCC on the ELISA plate and binding the N-terminally biotinylated A $\beta$ - peptides via a spacer peptide (Biotin-(Gly)<sub>5</sub>- A $\beta$  peptides), using of an antibiotin detection antibody. No anti-HCC or anti-A $\beta$  antibody was used to exclude a possible interference of the antibody epitope with the binding sites of the HCC-A $\beta$  complex. Biotinylated peptide derivatives of full length A $\beta$ (1-40), A $\beta$ (12-40), A $\beta$ (17-28) and A $\beta$ (1-16) were tested in a comparative ELISA experiment (Figure 12a). All A $\beta$  peptides comprising the HCC-binding epitope showed binding affinity to HCC, with A $\beta$ (17-28) having the highest affinity, while the N-terminal peptide A $\beta$ (1-16) did not show any binding. Thus, the ELISA results were in complete agreement with the mass spectrometric epitope identification.

Further comparative ELISA studies with the A $\beta$ (17-28) epitope were performed using the C-terminal HCC peptides identified by epitope excision-mass spectrometry, by coating the ELISA plate with intact HCC and the HCC(93-120), HCC(101-117), and HCC(101-114) fragments. The results confirmed the C-terminal HCC epitope, with the carboxy-terminal sequence being essential for binding affinity to A $\beta$  (Figure 12b).

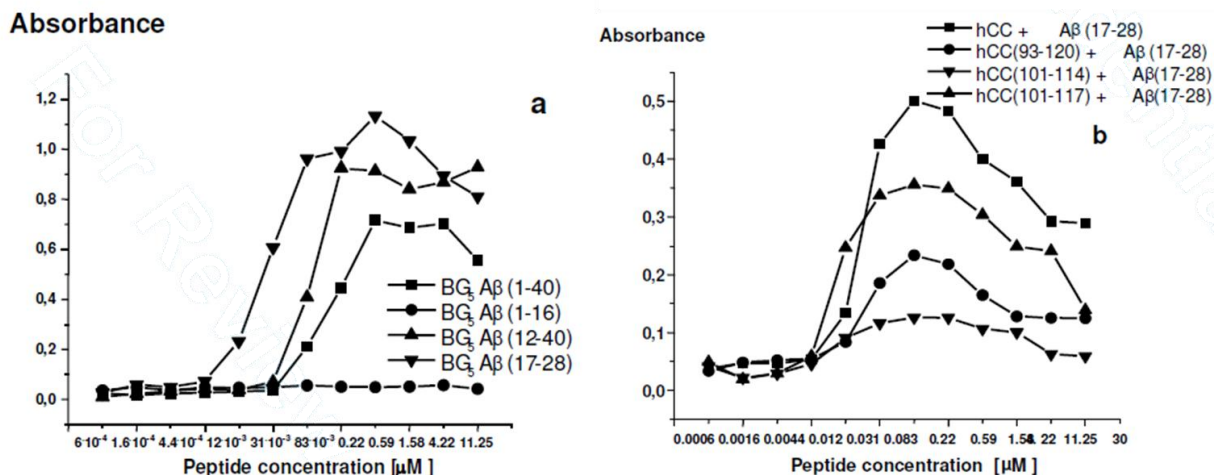


Figure 12: Antigen-antibody affinity binding for A $\beta$  peptides.

## 2.4 SAW bioaffinity studies of $\beta$ -amyloid and hCC peptides

The affinity interaction of the peptides was investigated using the SAW biosensor. The antibodies were immobilized on the active gold surface of the active gold surface of the biosensor chip and their interaction with peptides in dissolved in the liquid phase was observed. The studies show that the antibodies recognize  $\beta$ -amyloid peptides in concentration ranges from 1.22 nM to 2.5  $\mu$ M (table 2). These concentrations represent the minimum and the maximum limits of detection. The purpose was to demonstrate that the affinity between the antibody and peptides is detectable with the SAW biosensor, having the first peptide covalently immobilized and the second peptide free in the aqueous phase, but also the determination of the dissociation constant of the peptides involved. These limits of detection are needed to be determined in order to be possible the determination of the dissociation constant. For this determination is also necessary the existence of a minimum of 8 different concentration, being used in the present work 12 different concentrations between 1.22 nM and 2.5  $\mu$ M. For the affinity component of the study, the mass loading was the value found.



Table 2: Mass loading after affinity injection ( $A\beta$  peptides)

C [M]	hCC (101-117)			hCC (93-120)		
	$A\beta$ [1-40] [ $\mu\text{g cm}^{-2}$ ]	$A\beta$ [12-40] [ $\mu\text{g cm}^{-2}$ ]	$A\beta$ [17-28] [ $\mu\text{g cm}^{-2}$ ]	$A\beta$ [1-40] [ $\mu\text{g cm}^{-2}$ ]	$A\beta$ [12-40] [ $\mu\text{g cm}^{-2}$ ]	$A\beta$ [17-28] [ $\mu\text{g cm}^{-2}$ ]
$1.22 \cdot 10^{-9}$	-	0.0002751	-	0.0000005	0.0001254	0.0000075
$2.44 \cdot 10^{-9}$	-	0.0003112	-	0.0000636	0.0001517	0.0000251
$4.88 \cdot 10^{-9}$	-	0.0003224	-	0.0001009	0.0001942	0.0001690
$9.7 \cdot 10^{-9}$	-	0.0003368	-	0.0002598	0.000206	0.0001691
$19.5 \cdot 10^{-9}$	-	0.0003665	0.0000059	0.0002601	0.000207	0.0001863
$39 \cdot 10^{-9}$	0.00002636	0.0004354	0.0000486	0.0002599	0.0002607	0.0004583
$78 \cdot 10^{-9}$	0.00009711	0.0004809	0.0000832	0.0002598	0.0002923	0.0004584
$150 \cdot 10^{-9}$	0.00015905	0.0005246	0.0000911	0.000413	0.0003183	0.0005295
$300 \cdot 10^{-9}$	0.00028039	0.0005526	0.0001082	0.0005139	0.0003459	0.0006444
$625 \cdot 10^{-9}$	0.00032153	0.0005850	0.0001310	0.0005824	0.0003652	0.0007659
$1.25 \cdot 10^{-6}$	0.00044227	0.0006069	0.0001809	0.0005821	0.0003826	0.0009231
$2.5 \cdot 10^{-6}$	0.00050948	0.0007108	0.0003891	0.0008564	0.0006333	0.0009622

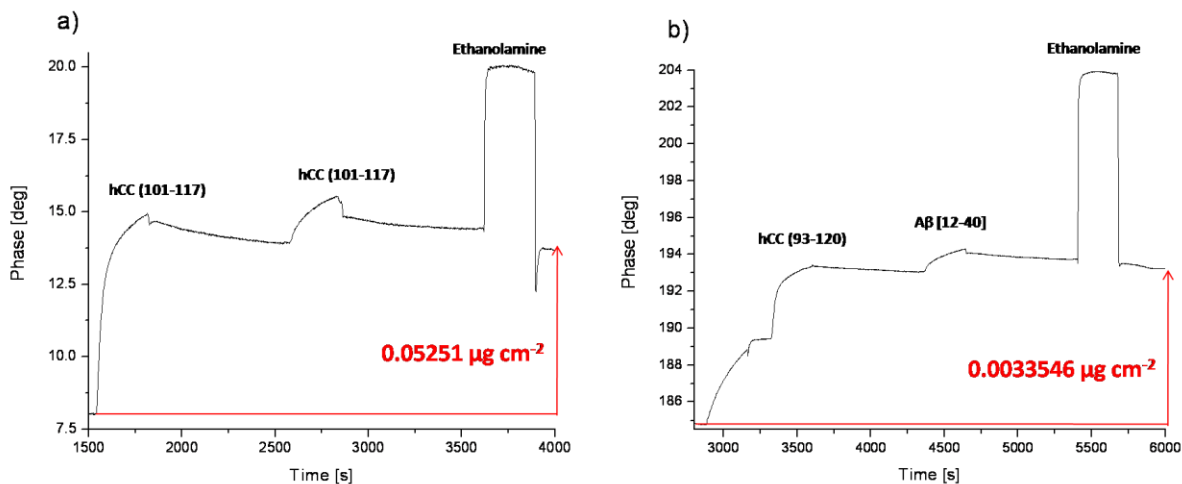


Figure 17: SAW binding curves referring to the immobilization of hCC a) (101-117) and b) (93-120) on the surface of the chip.

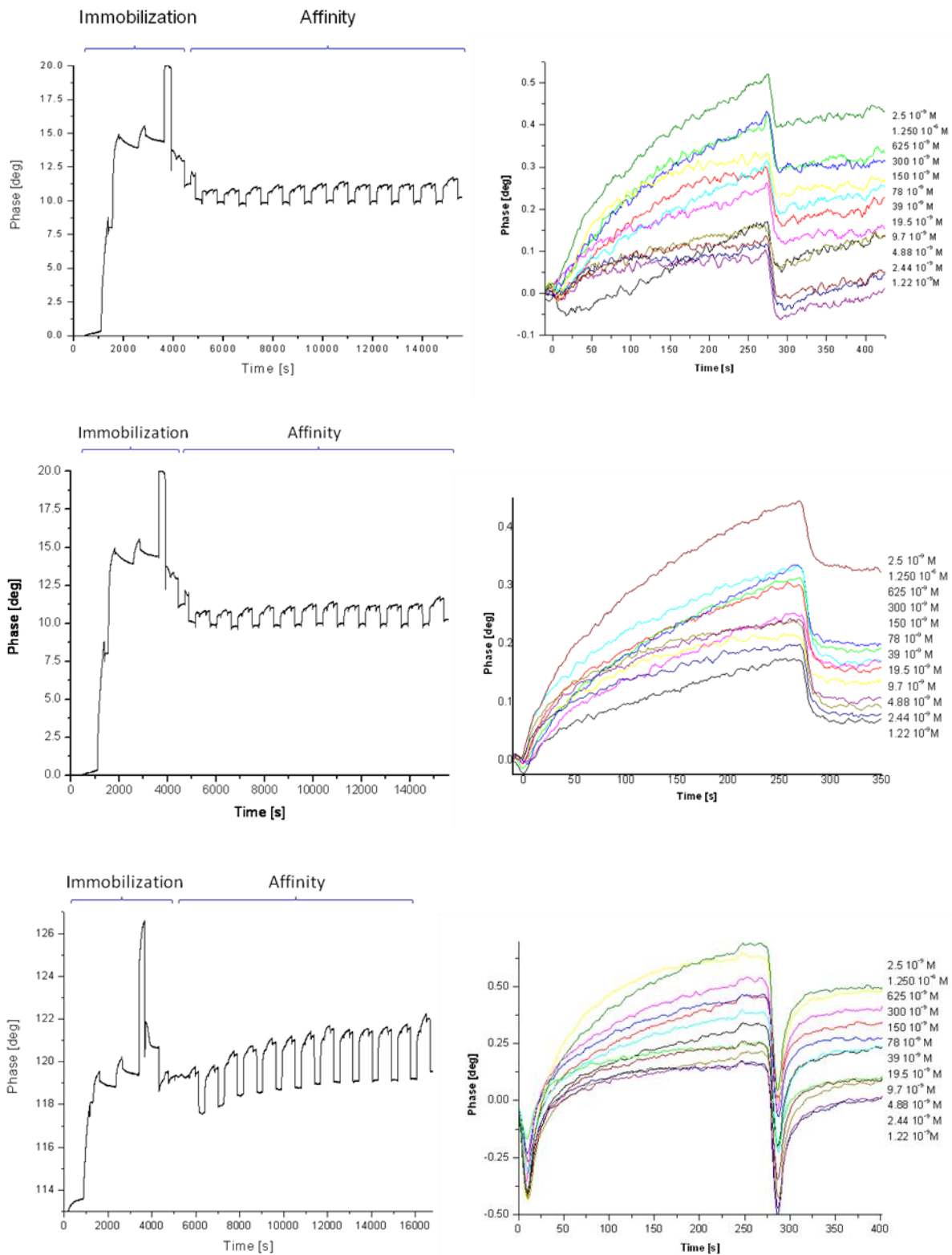
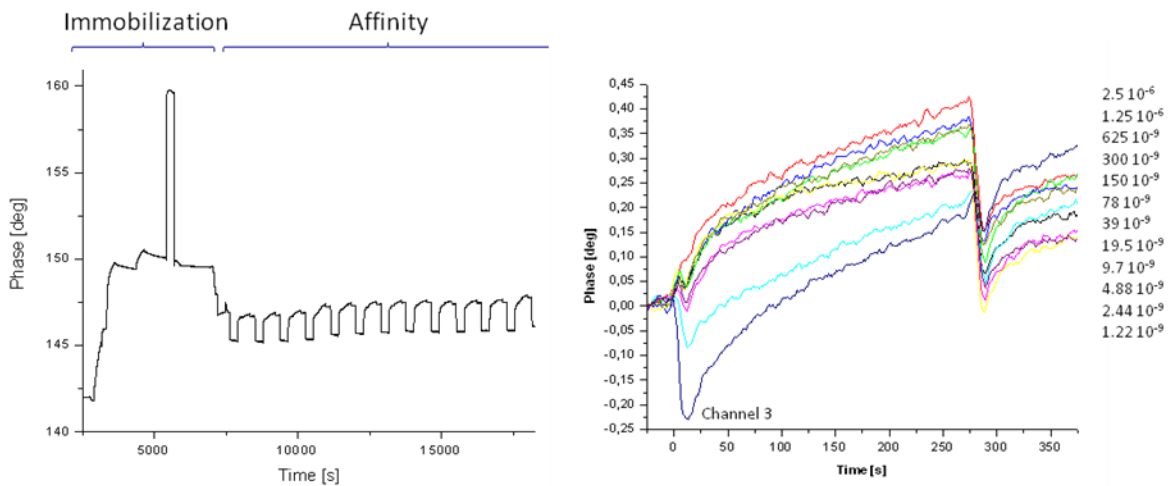
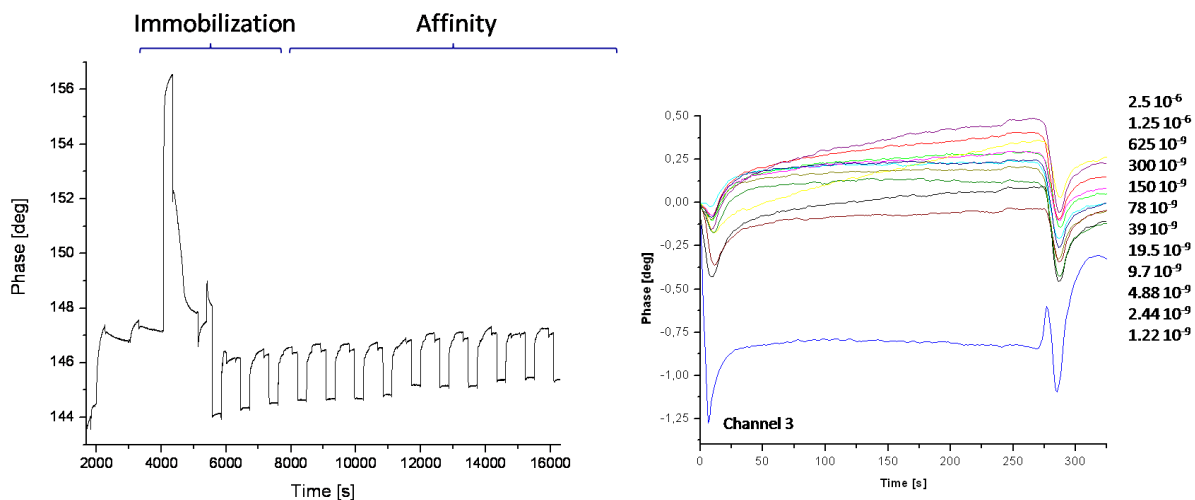


Figure 18: SAW binding curves referring to the: on the left the complete spectra and on the right the

affinity component with all the injections overlapped. The immobilization was performed with HCC (101-117) and then, in this order, the affinity with A $\beta$  (1-40), A $\beta$  (12-40) and A $\beta$  (17-28).



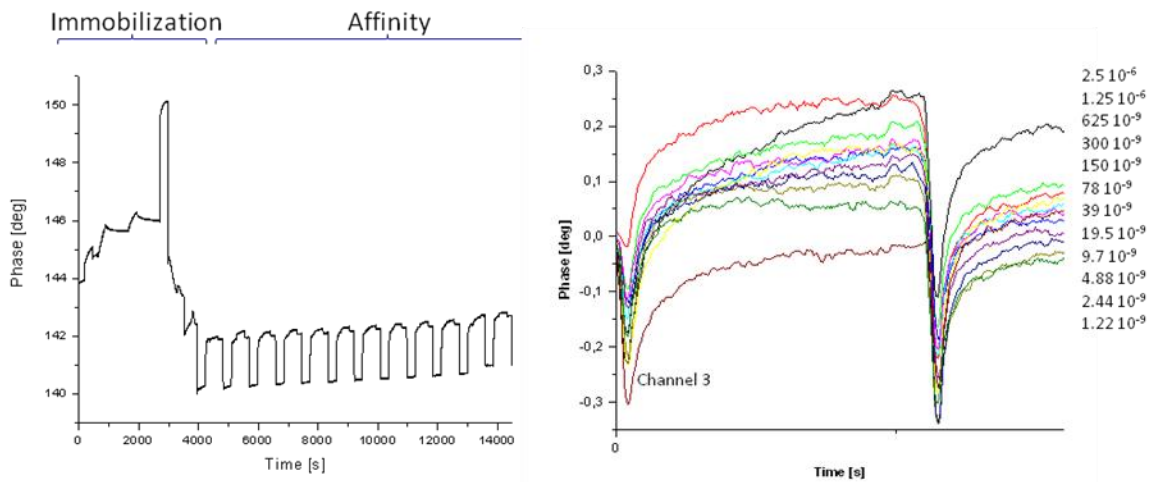
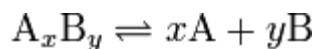


Figure 19: SAW binding curves referring to the: on the left the complete spectra and on the right the affinity component with all the injections overlapped. The immobilization was performed with HCC (93-120) and then, in this order, the affinity with A $\beta$  (1-40), A $\beta$  (12-40) and A $\beta$  (17-28).

## 2.5 Determination of dissociation constant of A $\beta$ and hCC peptides by SAW

A dissociation constant ( $K_d$ ) is a specific type of equilibrium constant that measures the propensity of a larger object to separate (dissociate) reversibly into smaller components, as when a complex falls apart into its component molecules, or when a salt splits up into its component ions. The dissociation constant is the inverse of the association constant.

For a general reaction:



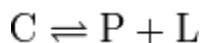
in which a complex  $A_x B_y$  breaks down into  $xA$  subunits and  $yB$  subunits, the dissociation constant is defined

$$K_d = \frac{[A]^x \times [B]^y}{[A_x B_y]}$$

where  $[A]$ ,  $[B]$ , and  $[A_x B_y]$  are the concentrations of A, B, and the complex  $A_x B_y$ , respectively.

The dissociation constant is commonly used to describe the affinity between a ligand (L) (such as a drug) and a protein (P) i.e. how tightly a ligand binds to a particular protein. Ligand-protein affinities are influenced by non-covalent intermolecular interactions between the two molecules such as hydrogen bonding, electrostatic interactions, hydrophobic and Van der Waals forces. They can also be affected by high concentrations of other macromolecules, which causes macromolecular crowding.[1][2]

The formation of a ligand-protein complex (C) can be described by a two-state process



the corresponding dissociation constant is defined

$$K_d = \frac{[P][L]}{[C]}$$

where [P], [L] and [C] represent the concentrations of the protein, ligand and complex, respectively.

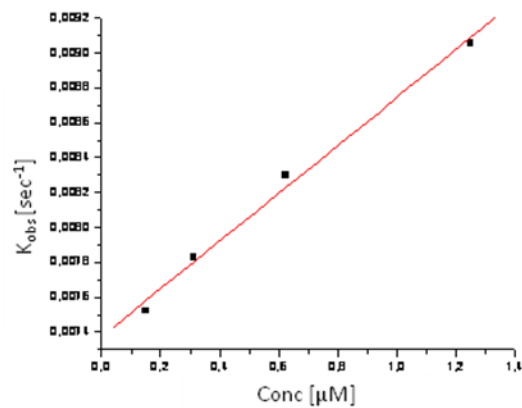
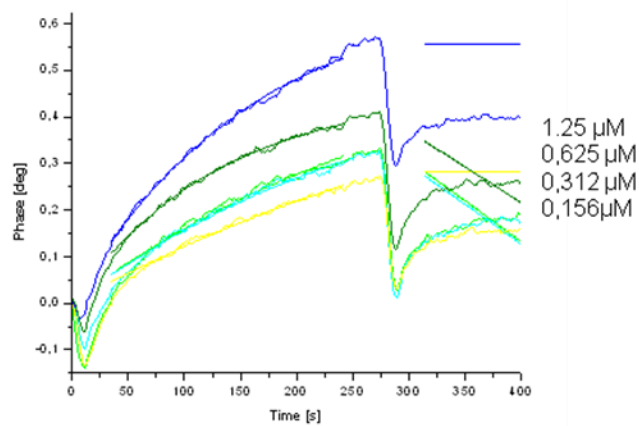
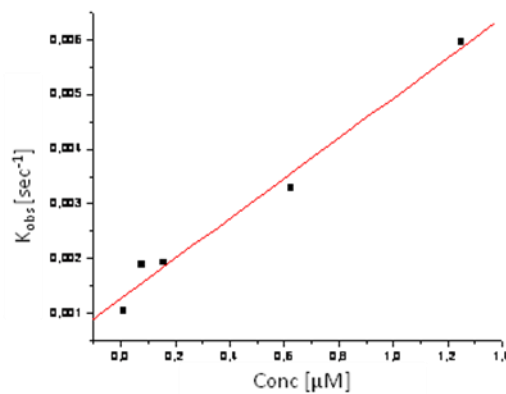
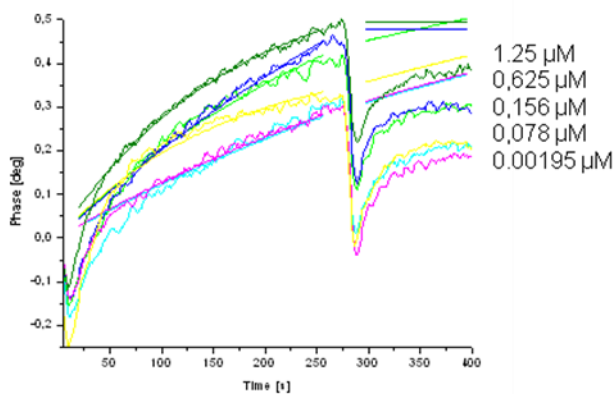
The dissociation constant has molar units (M), which correspond to the concentration of ligand [L] at which the binding site on a particular protein is half occupied, i.e. the concentration of ligand, at which the concentration of protein with ligand bound [C], equals the concentration of protein with no ligand bound [P]. The smaller the dissociation constant, the more tightly bound the ligand is, or the higher the affinity between ligand and protein. For example, a ligand with a nanomolar (nM) dissociation constant binds more tightly to a particular protein than a ligand with a micromolar ( $\mu$ M) dissociation constant.

The dissociation constant for a particular ligand-protein interaction can change significantly with solution conditions (e.g. temperature, pH and salt concentration). The effect of different solution conditions is to effectively modify the strength of any intermolecular interactions holding a particular ligand-protein complex together.

Knowing this, it is possible to determine the dissociation constants by using all the data resulting from the 12 different concentrations and the 5 channels that constitute the chip. The values presented result from the average of these 5 channels.

Table 3: Dissociation constants determined using SAW Biosensor.

	$KD_{(Ab\ 1-40)} [\mu M]$	$KD_{(Ab\ 12-40)} [\mu M]$	$KD_{(17-28)} [\mu M]$
hCC [101-117]	1,366	1,045	0,228
hCC [93-120]	0,0652	2,04	1,77



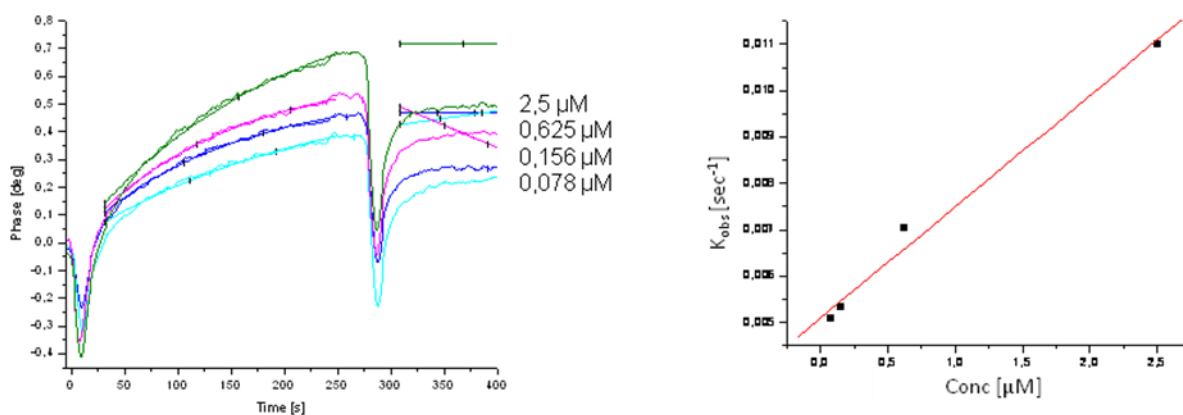
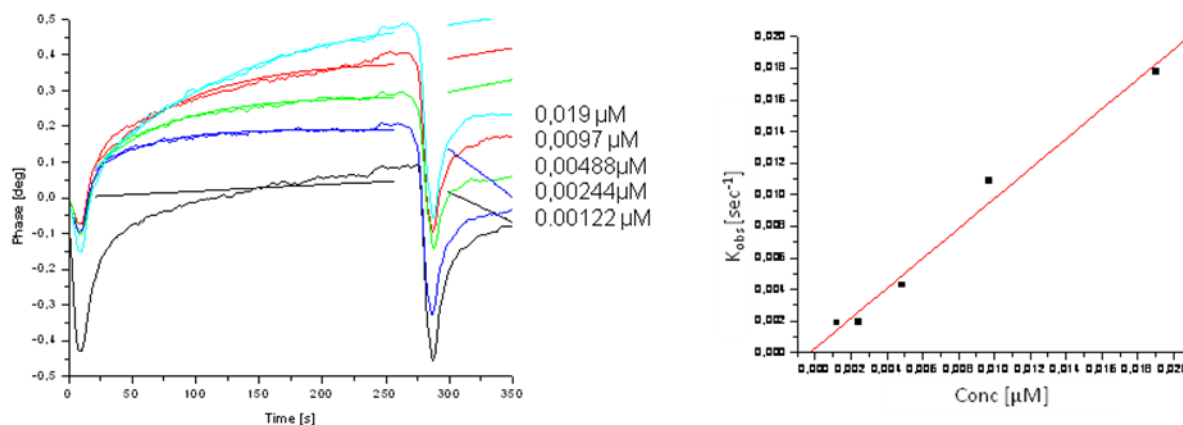


Figure 20: SAW binding curves referring to the: on the left the affinity spectra with the fitting parameters of the best values found among the different 1 concentrations used in the beginning, and on the right the linear regression that give the  $K_{obs}$  value which is used to determine the dissociation constant using the equations previously given. In this order, hCC (101-117) with A $\beta$  (1-40), A $\beta$  (12-40) and A $\beta$  (17-28).



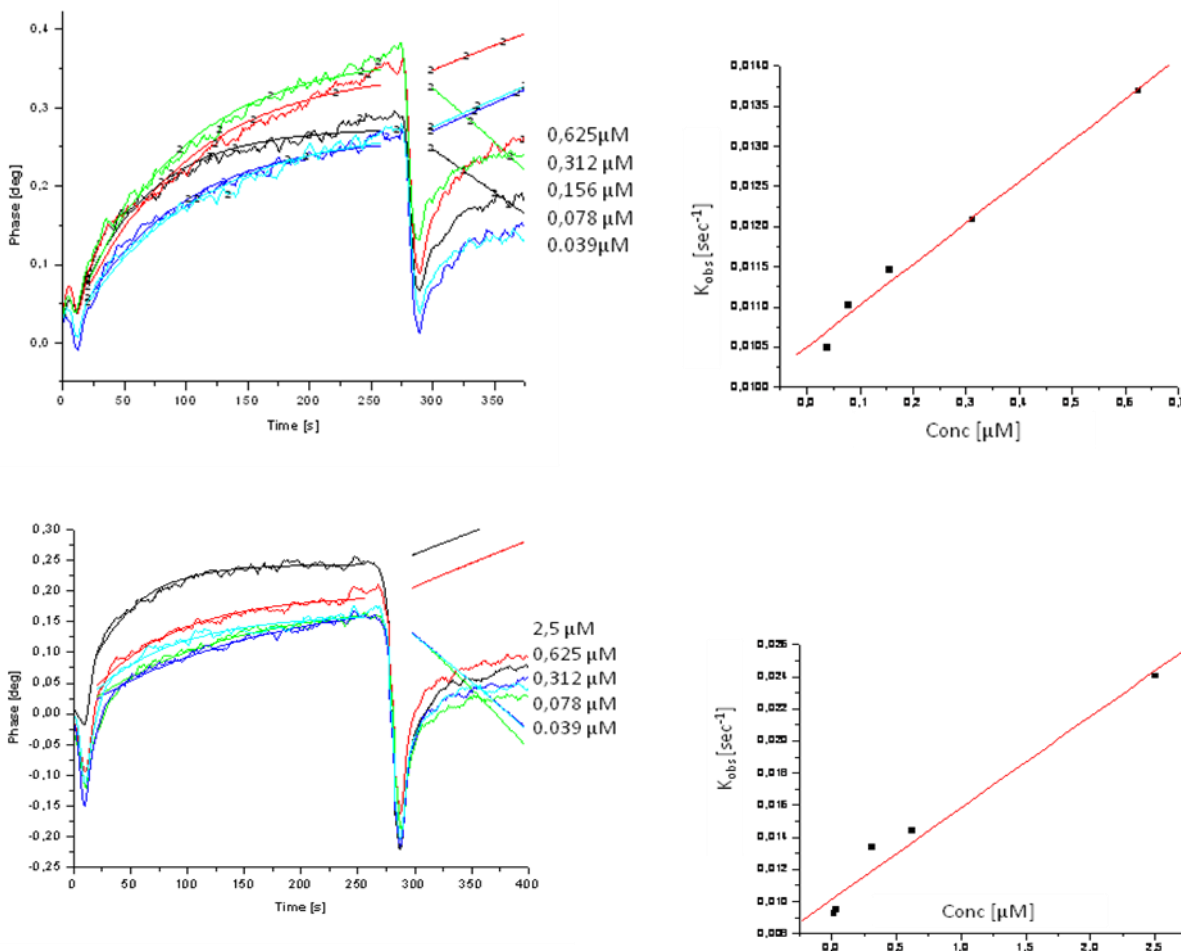


Figure 21: SAW binding curves referring to the: on the left the affinity spectra with the fitting parameters of the best values found among the different 1 concentrations used in the beginning, and on the right the linear regression that give the  $K_{obs}$  value which is used to determine the dissociation constant using the equations previously given. In this order, hCC (93-120) with Aβ (1-40), Aβ (12-40) and Aβ (17-28).

The values of  $k_d$  found are in agreement with the results obtained with the ELISA procedure and with some data already available in the literature. These data was obtained using a Biacore T100 instrument (Biacore SA, Uppsala, Sweden) with a KD of 3.9 μM for hCC (93-120) in affinity to Biotin-G5-Aβ(1-40), which is a positive reference point.



## 2.6 Inhibition of A $\beta$ -fibril formation by C-terminal HCC epitopes.

Inhibition studies of A $\beta$ -oligomerisation and fibril formation were performed with intact HCC in comparison with the C-terminal HCC epitope as shown in Table 2, using an *in vitro* assay of A $\beta$ - oligomerisation. [25] For formation of A $\beta$ -oligomers, A $\beta$ (1-40) was first dissolved in 100 % TFE to ensure re-formation of monomers, and the sample then lyophilized and redissolved in DMSO. The samples were then diluted to a final peptide concentration of 100  $\mu$ M in 50 mM phosphate buffer, pH 7.4, and a 10 % final DMSO, and A $\beta$ (1-40) with and without HCCepitope peptides incubated at 37 °C for up to 76 hours. Prior to analysis by SDS-PAGE, the samples were centrifuged at 13,000 x g for 5 min and then lyophilized. These comparative analyses clearly showed a time-and concentration-dependant, inhibitory effect of the HCC epitope peptides on the formation of A $\beta$ -oligomer aggregates, with highest relative effect obtained for the HCC (101-117)-peptide (Table 4). Thioflavine T (ThT) is a dye common used to visualize the amyloid fibrils. For the free dye excitation and emission occur at 385nm and 445 nm; for the bounded – excitation and emission occur at 450nm and 482nm (Figure 22).

Table 4: Relative inhibition (inhibition of oligomer bands) of A $\beta$ - fibril formation by HCC-epitope peptides after 72 hrs.

HCC-Peptide / A $\beta$ peptide %	HCC-epitope ( $\mu$ M)	% Fibril inhibition
HCC(93-120) / A $\beta$ (1-40) HCC(93-120)/ A $\beta$ (1-40)	10	10
HCC(101-117)/ A $\beta$ (17-28)	10	12
HCC(101-117)/ A $\beta$ (17-28)	100	51

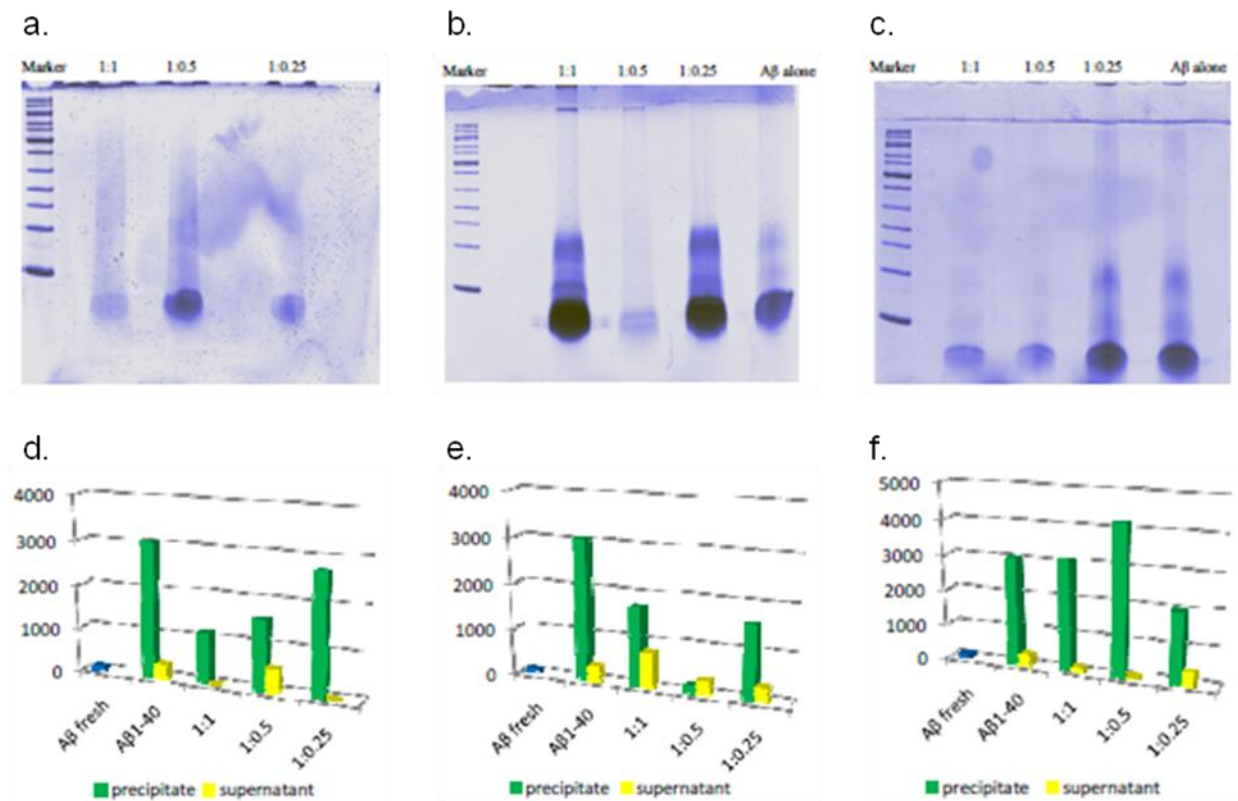


Figure 22: Relative inhibition (inhibition of oligomer bands) of A $\beta$ -fibril formation by HCC-epitope peptides after 72 hrs, with the respective information from the thioflavin assay. a. and d. as the combination of A $\beta$  (1-40) with hCC (93-120), b. and e. as the combination of A $\beta$  (1-40) with hCC (101-117); and c. and f. as the combination of A $\beta$  (17-28) with hCC (101-117).

The better experimental results are observed for Thioflavin T test comparing to gel electrophoresis. A $\beta$  (1-40) with hCC (93-120) in 1:1, 1:0.5 and 1:0.25 molar ratios shows clearly an inhibition process and it is dependent of the hCC concentration – the best inhibition process was observed in the molar ratio 1:1. Also A $\beta$  (1-40) with hCC (101-117) in 1:1, 1:0.5 and 1:0.25 molar ratio shows inhibitory effect but we cannot see the dependence on the hCC concentration. For A $\beta$  (17-28) with hCC (101-117) in 1:1, 1:0.5 and 1:0.25 molar ratio the Tris-PAGE shows clearly the inhibition dependence on the molar ratio.

## 2.7 Mass spectrometry.

MALDI-TOF MS analyses were carried out on a Bruker (Bruker Daltonics, Germany) Biflex ITM linear TOF mass spectrometer equipped with a nitrogen UV laser ( $\lambda = 337$  nm) and a dual channel plate detector, at conditions as previously described.<sup>17</sup> Samples were dissolved in 0.1 % trifluoroacetic acid and desalted using the Zip-Tip procedure. High resolution FTICR- mass spectrometry was performed with a Bruker (Bruker Daltonics, Bremen, Germany) APEX II FTICR instrument equipped with an actively shielded 7T superconducting magnet, a cylindrical infinity ICR analyzer cell, and an external Bruker Apollo-II nano-electrospray ion source.<sup>40</sup> Sample preparation of HCC- A $\beta$ -epitope complexes was carried out with 10  $\mu$ L aliquots of freshly prepared solutions of A $\beta$ (17-28) (100  $\mu$ M; Mr 1323.68) in deionised water, which were added to 10  $\mu$ L of an equimolar solution of HCC(101-117) or HCC(93-120) in 0.5 mM ammonium acetate, pH 6. After incubation of the HCC-A $\beta$ - peptide complex for three hrs at 25  $^{\circ}$ C, the solution was infused in the Apollo-II electrospray ionisation source at a flow rate of 4  $\mu$ L/min. FTICR Mass spectra were obtained by accumulation of 32 single scans, with the capillary exit voltage set to 50 V for ion desolvation external accumulation of ions in a radio frequency-only hexapole for 0.05 s before transfer into the ICR cell. The capillary voltage was adjusted between 960 and 1120 V until a stable spray was obtained. Other experimental conditions were: Setting of skimmer 1, 15; setting of skimmer 2,7; RF Amplitude, 600; ionization pulse time, 2 ms; mass resolution was approximately 150000. Acquisition of spectra was carried out with the Bruker Daltonics Software XMASS and corresponding programmes for mass calculation, data calibration, and processing.

Abnormal accumulation of  $\beta$ -amyloid peptide ( $A\beta$ ) into extracellular toxic plaques in the brain is responsible for the neurodegeneration and resulting dementia in Alzheimer's disease (AD). Therefore,  $A\beta$  represents an important molecular target for intervention in AD, and agents that can prevent its formation and accumulation or stimulate its clearance might be of therapeutic benefit. The immunological approach to the treatment of AD involves either stimulating the host immune system to recognize and attack  $A\beta$  or providing passively pre-formed antibodies. It has been shown that active immunization with  $A\beta$  (1-42) in transgenic mouse models of AD reduces both the accumulation of  $A\beta$  plaques in brain and associated cognitive impairment. However, a therapeutic trial of immunization with  $A\beta$  (1-42) in humans was discontinued due to the significant toxic side effects such as meningo-encephalitic cellular inflammatory reactions.

Human cystatin C (HCC) is an ubiquitous protease inhibitor in human body fluids which has a propensity to form  $\beta$ -amyloid ( $A\beta$ )-like fibrils and to coassociate with amyloidogenic proteins. A high (ca. 90%) proportion of patients with Alzheimer's disease (AD) has been diagnosed to also suffer from HCC amyloidosis, and a specific interaction between HCC and  $A\beta$  has been found. The molecular characterization of the  $A\beta$ -HCC epitope interaction structure provides lead structures of new neuroprotective inhibitors for AD and cystatin C amyloidosis therapy, and new tools for AD diagnostics.

Although the co-localisation of cystatin C and  $A\beta$  has been demonstrated in cerebral arteries of CAA patients [24] cerebral vasculature and brain parenchyma of AD patients [28] and in muscle cells of patients with age-dependent inclusion body myositis [25] the biological role of the HCC-  $A\beta$  interaction and mechanism of the HCC-  $A\beta$  co-aggregation has been hitherto unknown. In this study we investigated the binding epitopes between HCC and  $A\beta$  using a molecular affinity- mass spectrometry approach, [18] and present the first identification of the epitope sequences and interaction structure of the  $A\beta$ -HCC complex. The results of proteolytic excision- mass spectrometry show that the HCC binding site is located in the central region of  $A\beta$  within residues (17-28) which is critically important for the  $A\beta$  structure and aggregation. The  $A\beta$ -epitope identified comprises a part of the hydrophobic core at residues (17-22)

(LVFFA) and the  $\beta$ -turn for fibril formation located within residues (25-28).[30] Tycko et al. reported the residues (12-24) and (30-40) to be involved in the formation of the parallel  $\beta$ -sheet structure in fibrils.[31,32] The residues (25-35) are part of the highly hydrophobic C-terminal region of A $\beta$  which is crucial for oligomerization and fibrillogenesis,[33] while residues (17-21) have been proposed to be involved in side-chain interactions and are pivotal in the dimerisation of A $\beta$ .[30] Furthermore, it been suggested that the sequence KLVFFAE (16-22) has an inhibitory effect on fibril formation, indicating the importance of these residues for A $\beta$  assembly.[32,34] This region is very sensitive to single site mutations which cause significant changes of structure, aggregation and toxicity of A $\beta$ .[34-36] The HCC binding results confirm that HCC efficiently binds to this region, and by blocking the residues (17-28) can influence the A $\beta$  oligomerization, decreasing neurotoxicity and plaque formation. The HCC binding site in A $\beta$  identified here is different from that proposed by Sastre et al.,[25] as our results ascertain binding at the central domain of A $\beta$ , not at an N-terminal sequence as previously suggested.

The observed blocking of HCC binding to A $\beta$  by an anti-A $\beta$ (1-17) antibody may be well explained by steric hindrance of HCC access to the binding site starting at Leu-17. Selenica et al. showed that HCC reduced the *in vitro* formation of soluble oligomers and protofibrils of A $\beta$ (1-42); however, HCC did not dissolve preformed A $\beta$ - oligomers.[23] Our results suggest that HCC is interacting only with monomeric A $\beta$ , and binding of the 120 aa protein to the central domain of A $\beta$  may effectively suppress aggregation by blocking the access to the hydrophobic C-terminal part of A $\beta$ , thus inhibiting interaction with a second A $\beta$  molecule. In preformed oligomers the hydrophobic core is involved in A $\beta$ -A $\beta$  interactions thus blocking the access of HCC. This result is in full agreement with the hypothesis that the presence of HCC in A $\beta$  solution can decrease oligomerisation<sup>25</sup> and slow down the aggregation process. The HCC binding site in A $\beta$  identified here is localised in a similar position to the A $\beta$ epitope recognised by physiological A $\beta$ -autoantibodies in human serum which recognise a specific C-terminal domain of A $\beta$  and seem to play a neuroprotective role in the oligomerisation of A $\beta$ .[16] A similar, neuroprotective effect may be suggested for the HCC binding to A $\beta$ , in contrast to the plaque-specific effect of A $\beta$ -antibodies obtained by active immunisation, that target an

---

N-terminal A $\beta$ -epitope.<sup>12</sup> The A $\beta$ - binding site identified in HCC, residues (101-117) is located in the Cterminal part within the L2 loop and  $\beta$ 5 strand of HCC which comprise the external part of the protein and are exposed to the environment.[27] The C-terminal binding epitope enables interaction of the A $\beta$  peptide with the L2- $\beta$ 5 part without any restriction. The identification of the binding site in HCC may be of high importance for oligomerisation and fibrillisation studies of HCC and its amyloidogenic mutant L68Q which, due to its structural similarity to HCC [20,25] can be assumed to have a similar binding epitope for A $\beta$ . The knowledge of the binding epitope may be used for future *in vitro* studies of HCC fibril formation, since fibrils can be easily formed with the L68Q HCC mutant by 3D domain swapping, but not by native HCC. In a model postulated by Jaskolski [29] the A $\beta$  binding site is located in the center of the fibrils which would provide the opportunity to disturb the interaction between cystatin molecules by binding of A $\beta$  to the C-terminal part of monomeric HCC. Here, the HCCepitope identified could be used as a new template for designing efficient inhibitors for amyloid angiopathy related to cystatin C oligomerisation.

The interaction of HCC with A $\beta$  may be an important neuroprotective mechanism in brain, and may attenuate the oligomerisation of A $\beta$  and play a regulating role in A $\beta$  amyloidogenesis. The identification of the binding epitope of HCC in the central domain of A $\beta$  confirmed the importance of this protease inhibitor for the aggregation process and amyloidogenesis, since blocking the hydrophobic core may inhibit A $\beta$  oligomerisation and regulate fibril production. On the other hand, the identification of the binding site in HCC should be of importance for oligomerisation studies of cystatin C, and new oligomerisation inhibitors may be designed based on the HCC-epitope.[37,38] It seems somewhat paradox that interaction of two potentially amyloidogenic molecules might give a lead to control or inhibit neuropathological changes in amyloidogenic diseases.

### 3. EXPERIMENTAL PART

#### 3.1 Materials and reagents

The following commercial available reagents were used in the present work:

Antibodies: anti-A $\beta$  (1-16) antibody (clone 6E10) and anti-A $\beta$  (17-24) antibody (clone 4G8): Chemicon (Millipore); labeled goat anti-mouse IgG: Jackson ImmunoResearch; Coomassie Brilliant Blue G250, Tween-20 (Polyoxyethylensorbitanmonolaureat): Sigma; deionisate water MilliQ (MQ): Millipore; T-buthylmethyleter (99%), diethylether (99%), dimethylformamide (DMF, 99.8%), N-Methylmorpholine (NMM 99.5% p.a.), piperidine (99%), trifluoroacetic acid (TFA, 99 % p.a.), triisopropylsilane (97%): Fluka

The amino acids (N- $\alpha$  Fmoc protected), TGR resin and the activator Benzotriazol-1-yl-N-oxy-tris-pyrrolidino-phosphonium-hexafluoro-phosphat (PyBOP) used for peptide synthesis: NovaBiochem.

Hydrochloric acid (37% p.a.), sulfuric acid (98%), soium hydroxide (99%), acetic acid (100%) ethanolamine (99%), Trizma base (2-amino-2-hidroxymethyl-1,3-propandiol, 99,9%) sodium dihydrogen phosphate monohydrate (NaH<sub>2</sub>PO<sub>4</sub>, 99.5%), sodium acetate trihydrate (99.5%), hydrogen peroxide (30%), glycine (>99%), N-Hydroxysuccinimid (NHS): Merck; ethanol (99.8% p.a.), disodium hydrogen phosphate-2-hydrate (Na<sub>2</sub> HPO<sub>4</sub>, 99.5%), Riedel-de Haen; acetonitrile (CAN, 100%, p.a.): Roth; diethanolamine (min. 98%), 1-Ethyl-3-[3-dimethylaminopropyl]carbodiimide Hydrochloride (EDC): Sigma.

#### 3.2 Solid phase peptide synthesis

Solid phase peptide synthesis is a time saving approach to obtain high-yelds of high-purity peptides. It was first introduced in 1963 by Merrifield [59] and since then has

become a widely used method for the small scale peptides synthesis. The method consists of a cyclic repetition of simple chemical reactions which leads to the successive addition of  $\alpha$  amino acids into a chain anchored to an insoluble resin support. The main advantage in using the insoluble resin support is the fast and complete separation of the reaction products from the reaction mixture. Further, this allows the use of great excess of reactants, which increases the yield. In present work SPPS was employed for the synthesis of A $\beta$  and HCC peptides, using the Fmoc strategy [60, 61]. This implies the use of 9-fluorenylmethoxycarbonyl as amino-protecting group and other compatible protecting groups for the reactive side chains. All peptides were synthesized on a NovaSyn TGR resin (Figure 29). Before starting the synthesis, the resin was washed with 50 mL of DMF and allowed to "swell".

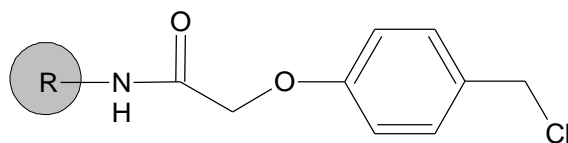


Figure 29: NovaSyn® TGR-resin from Novabiochem. PEG is the polyethyleneglycol spacer between the resin and the polystyrene matrix.

The synthesis were performed on a semiautomated peptide synthesizer EPS 221 from Abimed, Germany. The following  $\alpha$ -Fmoc protected amino acids were used in five-fold molar excess:  $\alpha$ -Fmoc-L-Alanine (Fmoc-Ala-OH),  $\alpha$ -Fmoc-S-trityl-L-Cystein (Fmoc-Cys(Trt)-OH),  $\alpha$ -Fmoc-L-Aspartic-acid- $\beta$ -t-butylester (Fmoc-Asp(OtBu)-OH),  $\alpha$ -Fmoc-L-Glutamicacid- $\gamma$ -t-butylester (Fmoc-Glu(OtBu)-OH),  $\alpha$ -Fmoc-L-Phenilalanine (Fmoc-Phe-OH),  $\alpha$ -Fmoc-Glycine (Fmoc-Gly-OH),  $\alpha$ -Fmoc-N-im-trityl-L-Histidine (Fmoc-His(Trt)-OH),  $\alpha$ -Fmoc-L-Iso-Leucine (Fmoc-Ile-OH),  $\alpha$ -Fmoc-N $\epsilon$ -t-Boc-L-Lysine (Fmoc-Lys(Boc)-OH),  $\alpha$ -Fmoc-N $\beta$ -trityl-L-Asparagine, (Fmoc-Asn(Trt)-OH),  $\alpha$ -Fmoc-L-Proline (Fmoc-Pro-OH),  $\alpha$ -Fmoc-N $\gamma$ -trityl-L-Glutamine (Fmoc-Gln(Trt)-OH),  $\alpha$ -Fmoc-NG-2,2,4,6,7-pentamethyl-dihydrobenzofuran-6-sulfonyl-L-Arginine (Fmoc-Arg(Pbf)-OH),  $\alpha$ -Fmoc-O-t-butyl-L-Seine (Fmoc-Ser(tBu)-OH),  $\alpha$ -Fmoc-O-t-butyl-L-Threonine (Fmoc-Thr(tBu)-OH),  $\alpha$ -Fmoc-L-Valine (Fmoc-Val-OH),  $\alpha$ -Fmoc-N-in-t-Boc-L-Tryptophan (Fmoc-Trp(Boc)-OH).



The main steps followed during a synthesis cycle are: a) the deprotection of the  $\alpha$ -amino group with 2% DBU and 10% piperidine in DMF for 5 minutes; the side products dibenzofulvene is scavenged by the piperidine and removed in the subsequent washing step; b) washing with DMF; c) activation of the amino acid with 0.9 M PyBOP and 1.3 M NMM in DMF; d) washing with DMF; e) coupling of the activated amino acid on the resin for 30 minutes; the coupling and the subsequent washing step are repeated for every amino acid of the sequence (Figure 30). In the end the last amino acid is also deprotected and the peptide is then cleaved from the resin with 95% TFA as cleavage reagent, 2.5% triethylsilan and 2.5% deionized water for 3 hours at room temperature. Then it was precipitated with 40 mL cold tert-butyl-methylether, filtered, dissolved in 5% acetic acid and lyophilized.

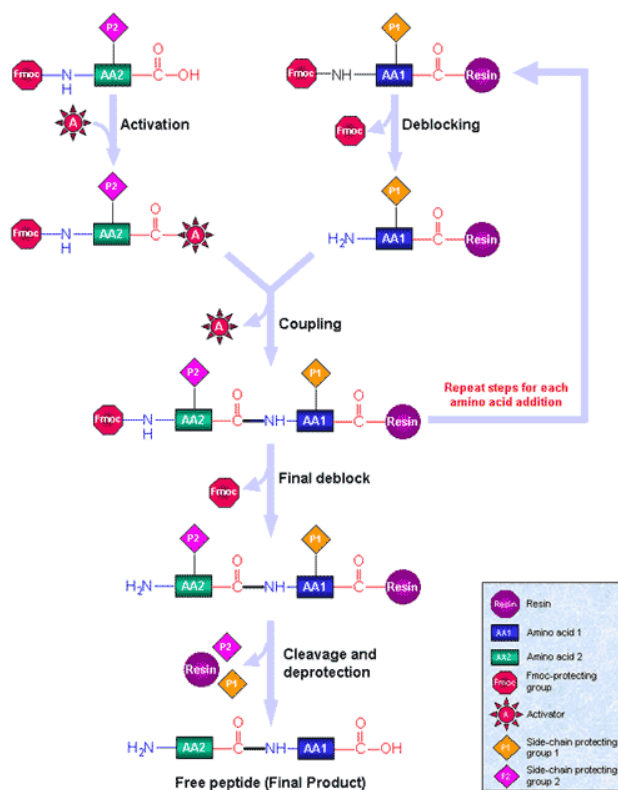


Figure 30: General scheme of solid phase peptide synthesis employing Fmoc\_/tBu strategy.

### 3.3 High performance liquid chromatography

High performance liquid chromatography (HPLC) is a separation method based on

sample partitioning between a coated silica solid phase and a mobile liquid phase. The term high-performance (also known as “high pressure”) refers to the speed and superior separation compared to agarose gel particules that were used before in column-chromatography. For peptide and protein separation the main type of HPLC used today is reversed-phase HPLC (RP-HPLC). This separation mode is based on acid nonpolar adsorption of peptides onto the hydrophobic stationary phase within the column. The peptides are then differentially released from the stationary phase as a function of increasing organic component in the liquid phase. The two major adjustments of the method that made it highly popular in the peptide and protein separation: the pore size of silica particles, which, increased from ~100 to ~300Å, had a dramatic effect on improving the separation of peptide, and the replacement of phosphoric with trifluoroacetic acid (TFA) as the ion-pairing agent, which was volatile and improved also the peptide separation. The sample is introduced into the HPLC column via a manual injector. The hydrophobic coating of the silica solid phase consists of saturated alkyl chains that interact with the hydrophobic moieties of the analyte. The elution is made with aqueous solvents containing TFA as ionic modifier to adjust the pH and CAN as an organic modifier is applied by using a two-phase mobile system:

Solvent A: 0.1% (v/v) TFA in MilliQ

Solvent B: 0.1% (v/v) TFA, 80% (v/v) acetonitrile in MilliQ

The solutions were thoroughly deaerated prior to use by sonication at low pressure (a vacuum was employed). The sample was dissolved in solvent A. To prevent column damage, the sample was centrifuged before injection. Analytical RP\_HPLC was performed on a UltiMate 3000 system (Dionex, Germering, Germany), equipped with LPG-3400A pumps, using a Vydac C4 column (250×4.6 mm I.D.) with 5 µm silica (300 Å pore size) (Hesperia CA). The chromatograms were recorded by UV detection at 220 nm, employing the VWD-3400 variable wavelength detector of the UltiMate system, with a flow cell of PEEKJ, 0.4 mm long and an internal volume of 0.7 µL. The fractions were collected with the FOXY Jr® automated fraction collector.

## 3.4 Gel Electrophoresis

### 3.4.1 SDS-PAGE

All peptide samples were analyzed by one-dimensional electrophoresis, to establish their constituency and purity. The electrophoresis was performed on polyacrylamide-gels, using also the SDS detergent in sample preparation. Proteins are biopolymers folded into compact structures held together by a variety of non-covalent interactions like salt bridges, hydrophobic interactions and hydrogen bonds. These interactions can be disrupted using SDS, a detergent that consists of a hydrophobic 12-carbon chain and a polar sulphated head. The hydrophobic chain intercalates into the hydrophobic parts of the protein, leaving the sulfate group on the surface of the protein. SDS coats the protein with a uniform "layer" of negative charges which replaces the net intrinsic charge of the native protein. Once the SDS treated samples are placed into a gel and an electric field is applied, the proteins migrate towards the anode and get separated depending only on their size. The size depending separation is achieved through the pores of the gel that allow the small molecules to travel faster than the big ones. The hydrogen bonding between the different amide groups present in the peptide chain plays a crucial role in the formation of protein secondary structures. High concentrations of urea interrupt these hydrogen bonds, rendering the polypeptides highly water-soluble. Urea achieves this through its strong dipole moment. However, because it is uncharged, urea does not migrate in electrical field and does not interfere with the results of the electrophoretic separation.

The gels were prepared using the mini-gel instrument MiniProtean from Bio-Rad.

In the table 5 are presented the solutions for the separation gel and stacking gel.

The separation gel buffer contains 0.5 M Tris, 0.4% SDS pH 6.8 and the stacking gel buffer contains 1.5M Tris, 0.4% SDS pH 8.8. The power/PAC 1000 instrument from Bio-Rad at constant current in two steps was used for gel electrophoresis.

- a. 60 V when the samples were in the stacking gel.
- b. 120 V when the samples were in the separation gel.

The molecular weight of the proteins was assigned using different markers.

Table 5: Solution volumes required for gel casting.

Solutions	Gel concentration		
	5%	12%	10%
<b>4x Stacking gel buffer</b>	2.5 mL	-	-
<b>4x Separation gel buffer</b>	-	6 mL	6 mL
<b>MilliQ</b>	5.8 mL	8.4 mL	10 mL
<b>Acrylamide solution</b>	1.7 mL	9.6 mL	8 mL
<b>10% Amonium peroxidsulphate</b>	85 µL	125 µL	125 µL
<b>N', N', N', N'- tetramethylethylenediamine</b>	20 µL	20 µL	20 µL

### 3.4.2 Staining of the gels with Coomassie Brilliant Blue

Coomassie Blue staining is based on the non-specifically binding of the dye Coomassie Brilliant Blue G250 to virtually all proteins in acid solutions. This binding results in a spectral shift from reddish-brown ( $\lambda$  465 nm) to blue ( $\lambda$  610 nm). Coomassie Blue binds roughly stoichiometrically to proteins, allowing densitometric determinations. The proteins are detected as blue bands on a clear background, after fixing the gel with trichloro-acetic acid (TCA) for obtaining maximum sensitivity. Staining solution was prepared from: acetic acid 10% (v/v); methanol 40% (v/v); Coomassie Brilliant Blue G-250 0.1% (w/v). After the gel was fixed for 30 minutes in fixing solution (12% TCA in MilliQ), it was left overnight in a mixture of 80 mL buffer (10%  $(\text{NH}_4)_2\text{SO}_4$ , 2%  $\text{H}_3\text{PO}_4$  in MilliQ) with 20 mL methanol and 2 mL Brilliant Blue G-Colloidal Concentrate, shaking. Afterwards the gel was washed with 25% methanol for 60 seconds and scanned with GS-710 Calibrated Imaging Densitometer from Bio-Rad. The image was acquired and saved with PD Quest software.

### 3.5 Inhibition assay of A $\beta$ -oligomerization by HCC peptides.

The gel was prepared using the mini-gel instrument MiniProtean from BioRad. Samples were dissolved in 50  $\mu$ L of running buffer (25 % glycerol, 4 % SDS, Coomassie) and added to the 12 % gel (8.4 mL MilliQ, 6 mL 4X separation buffer, 9.6 mL acrylamide solution, 125  $\mu$ L APS, 20  $\mu$ L TEMED). The power/PAC 1000 instrument from Bio-Rad at constant current was used for gel electrophoresis in two steps: (a) 60V when samples were in the stacking gel; (b) 120V when samples were in the separating gel.

Thioflavine T (ThT) is a dye common used to visualize the amyloid fibrils. For the free dye excitation and emission occur at 385nm and 445 nm; for the bounded – excitation and emission occur at 450nm and 482nm. For this experiment 100 $\mu$ M ThT solution was prepared in 50mM Glycine, pH 8.5. The samples (50 $\mu$ L of supernatant and 10 $\mu$ L of suspension) were loaded on a 96-well black plate together with 50 $\mu$ L ThT, and measured on PerkinElmer Wallac VICTOR2 E.L.I.S.A. reader. The results for each experiment are presented on graphs and they are average from two measurements.

### 3.6 Immunoanalytical Methods

#### 3.6.1 Enzyme linked immunosorbant assay (ELISA)

Indirect ELISA using antigen dilutions was carried out for the immunological characterization of A $\beta$  and HCC peptides. Ninety-six-well ELISA plates (Bio-Rad) were coated overnight at room temperature with 100  $\mu$ L/well of antigen (serial dilutions from 2.5  $\mu$ M to 0.00001  $\mu$ M of biotin G<sub>5</sub>A $\beta$ (...) peptides concentration). After coating, the wells were washed with 200  $\mu$ L/well PBS-T 0.05% Tween-20 v/v in PBS-phosphate buffer saline (Na<sub>2</sub>HPO<sub>4</sub> 5 mM, NaCl 150 mM, pH 7.) and the nonspecific adsorption sites were blocked with 200  $\mu$ L 5 % BSA for 2 h at RT. After incubation and washing steps, mouse anti-A $\beta$ (...), anti-A $\beta$  (...) were added to the plate. After another 2 h of incubation at room temperature the unbound first antibody was washed away and 100  $\mu$ L of peroxidase labeled goat anti-mouse IgG (Jackson Immuno Research) diluted 5000

times in 5% BSA was added to each well. After an additional incubation for 2 h, the wells were washed three times with PBS-T and once with 50 mM sodium phosphate-citrate buffer, pH 5. 100  $\mu$ L/well of 0.1% o-phenylenediamine dihydrochloride (OPD) in sodium phosphate-citrate buffer at 1 mg/mL and 2  $\mu$ L of 30% hydrogen-peroxide per 10 mL of substrate buffer was added to the plates. The absorbance was measured at  $\lambda = 450$  nm on a Wallac 1420 Victor<sup>2</sup> ELISA Plate counter (Perkin Elmer).

### 3.6.2 SAW Biosensor

The bioaffinity measurements were performed using a SAW biosensor K5 instrument from the firm Biosensor GmbH, Bonn. The instrument consists of the biosensor itself and an automated autosampler. The sensing surface consisting of gold is found on a small chip made of quartz. Before performing the actual measurements, the active surface of the chip has to be cleaned and then chemically modified, in order to permit the immobilization of the antibodies. The gold chips can be reused after a thorough cleaning of the surface. This is achieved by washing the chip using Piranha solution which consists of equal volumes of concentrated sulphuric acid (98%) and hydrogen peroxide (30%). Practically, the solution was made by mixing 1 mL of each reagent in a small glass recipient (the hydrogen peroxide was added first, then the acid). In the cold mixture (room temperature, 10 minutes after mixing) the chip was left for 45 minutes. After this, the chip was washed with MQ and ethanol, and then dried. Accordingly to the producer's specifications, the chips can be reused as many as 50 times, but in practice we observed a much faster degradation of the active surface (scratches and spots), after 10 to 20 cycles of use and cleaning. The formation of the self assembled monolayer (SAM) occurs through chemical adsorption from a solution containing compounds with thiol groups. A solution of 16-mercaptohexadecanoic acid 10  $\mu$ M is prepared by dissolving 5.77 mg of the acid in 2 mL of chloroform and ethanol, and then dried.

All reactions involved in the immobilization of the first partner of the affinity system are conducted in the micro-fluidic cell of the biosensors. The gold chip with a fresh SAM

build on its surface is inserted in the instrument and a flow of MQ is allowed to wash the chip. The flow rate is usually a small one, and kept relatively constant throughout the entire experiment. Typically used flow rates are 20 to 30  $\mu\text{L}/\text{min}$ . The reactants are added as solutions that are injected using the autosampler. In general, for the immobilization of a compound (antibody or protein) three injections are required. The first one contains the reactants for the activation, a mixture of 200 mM EDC (1-ethyl-3-(3-dimethylaminopropyl)carbodiimide) and 50 mM NHS (N-Hydroxysuccinimide) solutions, in a volumetric ratio of 1:1. Since EDC is quite unstable at room temperature, samples with weights close to 11.502 mg (quantity needed for 300 mL solution 200 mM) are weighted and then stored at  $-20\text{ }^\circ\text{C}$  in the freezer. Short before the injection, the solution is made by adding the required volume of PBS (used to insure the right pH for the reaction) over the EDC sample. The NHS is more stable than the EDC, but the same procedure is followed as for the EDC. The samples with weights close to 1.726 mg (quantity required for 300 mL solution 50 mM) are stored also in the freezer ( $-20\text{ }^\circ\text{C}$ ) or in the fridge ( $5\text{ }^\circ\text{C}$ ) and the solutions are made short before the injection by adding the right volume of PBS. Generally, in the autosampler was introduced a sample glass with 200  $\mu\text{L}$  mixture of both solutions and for the injection were use 150  $\mu\text{L}$ .

The second injection contains the compound to be immobilized (peptides, proteins and antibodies). Different concentrations and volumes have been tested in order to achieve a maximum quantity of compound on the chip. However, given the purpose of the work, the focus was to determine the best conditions for the immobilization of the antibodies. A maximum quantity of antibody on chip can be achieved by injecting 150  $\mu\text{L}$  (out of 200  $\mu\text{L}$  inserted in the autosampler) of a 200 nM antibody solution in MQ. With a molecular weight of ..., the solution was prepared diluting ...  $\mu\text{g}$  peptide in 200  $\mu\text{L}$  MQ. Practically we added 6  $\mu\text{L}$  stock solution of peptide (which had a concentration of 1  $\mu\text{g}/\mu\text{L}$ ) to 194 MQ. The third injection the function of capping all the activated carboxyl groups that did not reacted with the compound to be immobilized. It consisted of a 1 M solution of ethanolamine, brought to pH 8.5. From the 200  $\mu\text{L}$  inserted in the autosampler, were

injected only 100 or 120  $\mu$ . After the immobilization of a first compound, its affinity partner was also injected. This was done when the signal of the biosensor was equilibrated back after the change of the buffer from MQ (used during the immobilization) to PBS. For the study of the affinity interactions PBS was used as buffer in order to adapt the conditions of the experiment as close as possible to those of the physiological environment. For the injection of the affinity partner were also different concentrations and volumes used, according to the purpose of the experiment.

For attempting the coupling of the biosensor with the ESI-ion trap mass spectrometer, it was aimed to bind through affinity to the chip as much compound as possible through a single injection. For eluting the affinity bound compounds from the chip, we used acidic conditions, injecting for example glycine 50 mM (with an adjusted pH 2) or acetic acid 1% (pH 1.8). However, for disassociation of the antigen/antibody complexes we found the solution of HCl 0.1 M (pH 1.8) to be best suited. Active surface of a channel is 0.072  $\text{cm}^2$ . The quantity of bound compound to the chip can be evaluated from the measured phase shift (recorded with the K15 software) using the following sensitivity calibration factor:

$$515 = \varphi(^{\circ}) / (m(\mu\text{g}) \cdot A(\text{cm}^2))$$

### 3.6.3 ZipTip desalting and clean up procedure

The ZipTip desalting procedure was performed using ZipTip® C<sub>18</sub> and C<sub>4</sub> pipette tips from Millipore. The ZipTip pipette tips are modified pipette tips containing a small bed of reversed-phase chromatography media (0.6  $\mu\text{L}$ ) inside the cone end of the tip, with no dead volume. ZipTip C<sub>18</sub> pipette tips are to be used for peptides and low molecular weight proteins. The procedure was performed according to the instructions of the producer, following five major steps: wetting the chromatographic media, equilibration of the ZipTip pipette tip, binding of the peptides and/or proteins to ZipTip pipette tip, washing off of the impurities and salts, elution of the purified and



desalted protein/peptide sample. The used solutions are listed in Table 3.

Table 3: Solutions required for use with ZipTip pipette tips containing  $C_{18}$  media.

Solution	ZipTip $C_{18}$ Pipette Tips	
Wetting solution	100% ACN in MilliQ water	
Sample preparation	0.1% TFA in MilliQ water (final sample solution pH<4)	
Equilibration solution	0.1% TFA in MilliQ water	
Wash solution	0.1% TFA in MilliQ water	
Elution solution	for MALDI	0.1% TFA/50% ACN
	for ESI	2% acetic acid/50% methanol

### 3.6.4 ESI-Ion Trap-MS

All mass spectra were obtained using an ESI ion trap mass spectrometer Esquire 3000 plus from Bruker Daltonik (Bremen, Germany). The scheme of its build-up is presented in Figure 34.

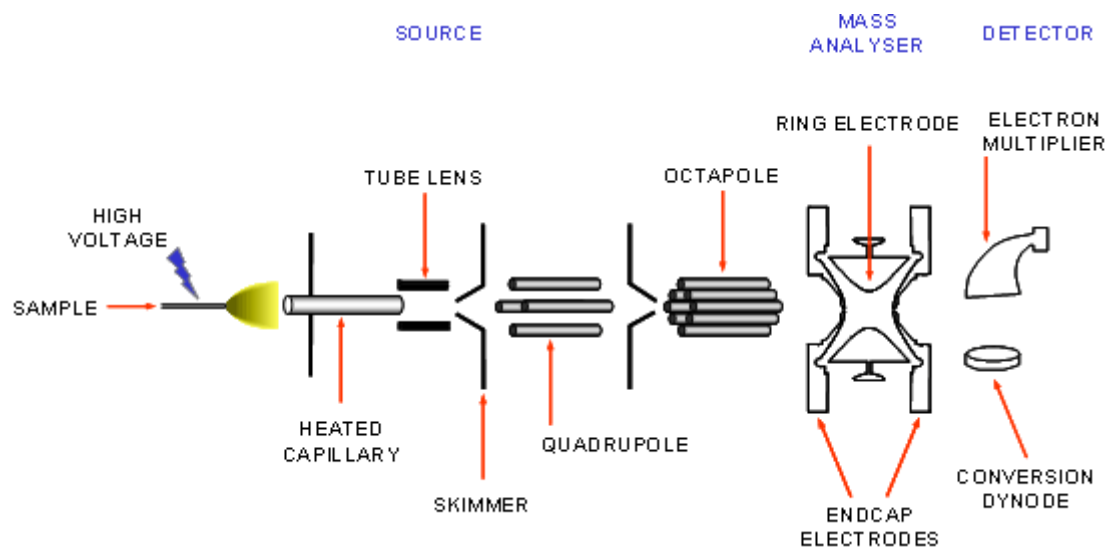


Figure 34: Schematic representation ESI ion trap mass spectrometer Esquire 3000 plus from Bruker. The ions are generated by the ESI source, are introduced in the mass spectrometer through a capillary, are

focused by two octopoles and then allowed to enter the ion trap. After being separated according to their  $m/z$  values, the ions exit the trap and reach the detector.

The A $\beta$  and HCC peptides, solubilized in 1% formic acid at a final concentration of 10  $\mu$ M, were measured through direct infusion with an Esquire 3000 Plus ion trap device. The instrument was controlled by the equireControl software. For the direct bioaffinity, a binary gradient system consisting of solvent A (0.3% formic acid, 5% acetonitrile) and solvent B (95% acetonitrile, 0.3% formic acid in water) was employed. All MS results were obtained using atmospheric pressure chemical ionization (APCI) in the positive ion mode. Mass spectra were recorded in the full scan mode, scanning from  $m/z$  100 to 3000. Ion source parameters were 15 psi nebulizer gas and 6L/min of drying gas with a temperature of 200 °C (Table 4).

Table 6: The ESI ion trap parameters:

<b>Parameter</b>	<b>Value</b>
<b>Target mass</b>	1000
<b>Compound stability</b>	100%
<b>Trap drive</b>	80%
<b>Nebulizer</b>	15 psi
<b>Dry gas</b>	6L/min
<b>Dry temperature</b>	200 °C
<b>Mode</b>	Positive
<b>Scann</b>	100-3000
<b>Average scans</b>	6

## 4.7 Computer programs

### 4.7.1 GPMAW

The software GPMAW 5.0 (General Protein/Mass Analysis for Windows) from Lighthouse Data, Denmark, was employed in the theoretical calculation of molecular

weight of the peptides and proteins. The program was able to calculate both the monoisotopic and average masses of the peptides or proteins having as input their sequence. It also allowed to modify the sequence adding different chemical modifications, e.g. to the side chain of the amino acid rest. It was also possible to predict the average and the monoisotopic values for the single and multiple charge ions. Another feature of GPMAW 5.0 is the prediction of the secondary structure and the hydrophobicity of a given protein or peptide sequence.

## 4. SUMMARY

Alzheimer's disease (AD) and AD-related neurodegenerative disorders have become the predominant form of progressive cognitive failure in elderly humans, a development presently accelerating due to the significant increase in life expectancy in the last decades. A major constituent of amyloid fibrils in brain of patients with AD and AD-related diseases, as well as in aged individuals without any neurological disorder is the  $\beta$ -amyloid polypeptide ( $A\beta$ ).  $A\beta$  arises from a large precursor, the amyloid precursor protein (APP); [1,2] it is produced by normal cells and detected as a circulating peptide in plasma and cerebrospinal fluid (CSF) of healthy humans.[3, 4]The accumulation of  $A\beta$ , a 39-42 amino acid proteolytic fragment of APP, in neuritic AD plaques is thought to be causative for disease progression. [3, 4]

Although amyloid plaques in brain of AD patients contain predominantly  $A\beta$ -aggregates, immunohistochemical studies have shown the co-deposition of several other proteins, such as the protease inhibitor cystatin C, apolipoprotein E, clusterin, transthyretin and gelsolin. [5-8] In particular, the presence of human cystatin C (hCC) in amyloid deposits has found much interest, [9, 10] and a wide spectrum of activities has been associated with hCC such as modulation of neuropeptide activation and neurite proliferation. [11, 12]

The 13 kDa protein hCC is the main cysteine protease inhibitor in mammalian body fluids [13, 14 ] and has been found with high concentrations in CSF. The presence of hCC in  $A\beta$ -plaques has been suggested to result from its binding to APP, or alternatively, hCC may bind to  $A\beta$  prior to the secretion or following the deposition in brain. [9] Sastre et al. found that the association of hCC with  $A\beta$  causes an inhibition of fibril formation, and suggested an N-terminal  $A\beta$ -sequence to be responsible for the interaction, with formation of a stoichiometric hCC-As complex. [11] The interaction of hCC with  $A\beta$  may be an important neuroprotective mechanism in brain, and may attenuate the oligomerisation of  $A\beta$  and play a regulating role in  $A\beta$  amyloidogenesis. The identification of the binding epitope of hCC in the central domain of  $A\beta$  confirmed the importance of this protease inhibitor for the aggregation process and

---

amyloidogenesis, since blocking the hydrophobic core may inhibit A $\beta$  oligomerisation and regulate fibril production.

Using proteolytic extraction and excision of the human cystatin C-A $\beta$ (1-40) immune complex (e.g. trypsin, Glu-C proteases) in combination with electrospray ionization (ESI)- and MALDI- mass spectrometry, the epitope was identified at the middle-carboxy terminal domain of A $\beta$ , A $\beta$ (17-28). An almost identical minimal epitope to that of the VHH-anti-A $\beta$ -antibody (A $\beta$ (17-24)) was found, which binds to a specific C-terminal domain of HCC, HCC(101-114) [1, 2]. The identified HCC epitope peptide was found to specifically inhibit A $\beta$ -oligomerization in vitro, in agreement with the A $\beta$ -epitope domain interfering with the A $\beta$ -aggregation. Other affinity studies using SAW and ELISA allowed to understand better the interaction between these two groups of peptides. The identified A $\beta$  and HCC epitopes and the study of their affinity represent new lead structures for designing neuroprotective inhibitors of the A $\beta$ -aggregation process, and for molecular AD diagnostics.

The discovery of soft ionization methods such as MALDI and ESI has the mass spectrometry analyses of biomacromolecules. Since then, mass spectrometry has become one of the most important analytical methods for the analysis of biopolymers. Biosensors have been recently developed as new analytical tools that rapidly found applications in the study of biomolecular interactions. The SAW biosensor is suitable to analyze samples in solution, being highly sensitive to mass loadings and viscosity changes. Therefore, the SAW biosensor is successfully used for affinity binding studies. However, a principal weakness of all bioaffinity methods is the lack of molecular structure information of ligand-binder interactions. The method was applied to several antigen-antibody systems related to a neurodegenerative disease of great impact worldwide, Alzheimer's disease). The antibodies were covalently immobilized on the surface of the chip used by the SAW sensor and the interactions with the antigens (peptide or protein) present in solution were determined.

---

Several A $\beta$  peptides were synthesized and their bioaffinity to HCC peptides was studied. The investigated antigen-antibody systems were: A $\beta$  (1-40) with HCC (93-120), A $\beta$  (12-40) with HCC (93-120), A $\beta$  (17-28) with HCC (93-120); A $\beta$  (1-40) with HCC (101-117), A $\beta$  (12-40) with HCC (101-117), and A $\beta$  (17-28) with HCC (101-117) as well as the inverse systems. The bioaffinities were comparatively investigated by ELISA and SAW, and the results were found to be in good agreement. It was demonstrated that all the systems (after a successful synthesis and purification) present affinity, and was possible to calculate all the constant dissociation basing on the affinity results.

## 5. REFERENCES

- (1) Glenner, G. G.; Wong, C. W. Alzheimer's disease and Down's syndrome: sharing of a unique cerebrovascular amyloid fibril protein. *Biochem Biophys Res Commun* **1984**, *122*, 1131-1135.
- (2) Hardy, J.; Selkoe, D. J. The amyloid hypothesis of Alzheimer's disease: progress and problems on the road to therapeutics. *Science* **2002**, *297*, 353-356.
- (3) Kang, J.; Lemaire, H. G.; Unterbeck, A.; Salbaum, J. M.; Masters, C. L. et al. The precursor of Alzheimer's disease amyloid A4 protein resembles a cell-surface receptor. *Nature* **1987**, *325*, 733-736.
- (4) Tanzi, R. E.; Gusella, J. F.; Watkins, P. C.; Bruns, G. A.; St George-Hyslop, P. et al. Amyloid beta protein gene: cDNA, mRNA distribution, and genetic linkage near the Alzheimer locus. *Science* **1987**, *235*, 880-884.
- (5) Calero, M.; Rostagno, A.; Frangione, B.; Ghiso, J. Clusterin and Alzheimer's disease. *Subcell Biochem* **2005**, *38*, 273-298.
- (6) Anderson, D. H.; Talaga, K. C.; Rivest, A. J.; Barron, E.; Hageman, G. S. et al. Characterization of beta amyloid assemblies in drusen: the deposits associated with aging and age-related macular degeneration. *Exp Eye Res* **2004**, *78*, 243-256.
- (7) Bard, F.; Cannon, C.; Barbour, R.; Burke, R. L.; Games, D. et al. Peripherally administered antibodies against amyloid beta-peptide enter the central nervous system and reduce pathology in a mouse model of Alzheimer disease. *Nat Med* **2000**, *6*, 916-919.
- (8) Schenk, D.; Barbour, R.; Dunn, W.; Gordon, G.; Grajeda, H. et al. Immunization with

---

amyloid-beta attenuates Alzheimer-disease-like pathology in the PDAPP mouse. *Nature* **1999**, *400*, 173-177.

(9) DeMattos, R. B.; Bales, K. R.; Cummins, D. J.; Dodart, J. C.; Paul, S. M. et al. Peripheral anti-A beta antibody alters CNS and plasma A beta clearance and decreases brain A beta burden in a mouse model of Alzheimer's disease. *Proc Natl Acad Sci U S A* **2001**, *98*, 8850-8855.

(10) Janus, C.; Pearson, J.; McLaurin, J.; Mathews, P. M.; Jiang, Y. et al. A beta peptide immunization reduces behavioural impairment and plaques in a model of Alzheimer's disease. *Nature* **2000**, *408*, 979-982.

(11) Hock, C.; Konietzko, U.; Streffer, J. R.; Tracy, J.; Signorell, A. et al. Antibodies against beta-amyloid slow cognitive decline in Alzheimer's disease. *Neuron* **2003**, *38*, 547- 554.

(12) McLaurin, J.; Cecal, R.; Kierstead, M. E.; Tian, X.; Phinney, A. L. et al. Therapeutically effective antibodies against amyloid-beta peptide target amyloid-beta residues 4-10 and inhibit cytotoxicity and fibrillogenesis. *Nat Med* **2002**, *8*, 1263-1269.

(13) Tian, X.; Cecal, R.; McLaurin, J.; Manea, M.; Stefanescu, R. et al. Identification and structural characterisation of carboxy-terminal polypeptides and antibody epitopes of Alzheimer's amyloid precursor protein using high-resolution mass spectrometry. *Eur J Mass Spectrom* (Chichester, Eng) **2005**, *11*, 547-556.

(14) Du, Y.; Dodel, R.; Hampel, H.; Buerger, K.; Lin, S. et al. Reduced levels of amyloid beta-peptide antibody in Alzheimer disease. *Neurology* **2001**, *57*, 801-805.

(15) Du, Y.; Wei, X.; Dodel, R.; Sommer, N.; Hampel, H. et al. Human anti-beta-amyloid antibodies block beta-amyloid fibril formation and prevent beta-amyloid-induced neurotoxicity. *Brain* **2003**, *126*, 1935-1939.



- (16) Dodel, R. C.; Du, Y.; Depboylu, C.; Hampel, H.; Frolich, L. et al. Intravenous immunoglobulins containing antibodies against beta-amyloid for the treatment of Alzheimer's disease. *J Neurol Neurosurg Psychiatry* **2004**, *75*, 1472-1474.
- (17) Stefanescu, R.; Iacob, R. E.; Damoc, E. N.; Marquardt, A.; Amstalden, E. et al. Mass spectrometric approaches for elucidation of antigenantibody recognition structures in molecular immunology. *Eur J Mass Spectrom (Chichester, Eng)* **2007**, *13*, 69-75.
- (18) Macht, M.; Fiedler, W.; Kurzinger, K.; Przybylski, M. Mass spectrometric mapping of protein epitope structures of myocardial infarct markers myoglobin and troponin T. *Biochemistry* **1996**, *35*, 15633-15639.
- (19) Levy, E.; Sastre, M.; Kumar, A.; Gallo, G.; Piccardo, P. et al. Codeposition of cystatin C with amyloid-beta protein in the brain of Alzheimer disease patients. *J Neuropathol Exp Neurol* **2001**, *60*, 94-104.
- (20) Rodziewicz-Motowidlo, S.; Wahlbom, M.; Wang, X.; Lagiewka, J.; Janowski, R. et al. Checking the conformational stability of cystatin C and its L68Q variant by molecular dynamics studies: why is the L68Q variant amyloidogenic? *J Struct Biol* **2006**, *154*, 68-78.
- (21) Calero, M.; Pawlik, M.; Soto, C.; Castano, E. M.; Sigurdsson, E. M. et al. Distinct properties of wild-type and the amyloidogenic human cystatin C variant of hereditary cerebral hemorrhage with amyloidosis, Icelandic type. *J Neurochem* **2001**, *77*, 628-637.
- (22) Levy, E.; Jaskolski, M.; Grubb, A. The role of cystatin C in cerebral amyloid angiopathy and stroke: cell biology and animal models. *Brain Pathol* **2006**, *16*, 60-70.
- (23) Selenica, M. L.; Wang, X.; Ostergaard-Pedersen, L.; Westlind-Danielsson, A.; Grubb, A. Cystatin C reduces the in vitro formation of soluble Abeta1-42 oligomers and protofibrils. *Scand J Clin Lab Invest* **2007**, *67*, 179-190.

- 
- (24) Vattemi, G.; Engel, W. K.; McFerrin, J.; Askanas, V. Cystatin C colocalizes with amyloid-beta and coimmunoprecipitates with amyloid-beta precursor protein in sporadic inclusion-body myositis muscles. *J Neurochem* **2003**, *85*, 1539-1546.
- (25) Sastre, M.; Calero, M.; Pawlik, M.; Mathews, P. M.; Kumar, A. et al. Binding of cystatin C to Alzheimer's amyloid beta inhibits in vitro amyloid fibril formation. *Neurobiol Aging* **2004**, *25*, 1033-1043.
- (26) Carrette, O.; Demalte, I.; Scherl, A.; Yalkinoglu, O.; Corthals, G. et al. A panel of cerebrospinal fluid potential biomarkers for the diagnosis of Alzheimer's disease. *Proteomics* **2003**, *3*, 1486-1494.
- (27) Janowski, R.; Kozak, M.; Jankowska, E.; Grzonka, Z.; Grubb, A. et al. Human cystatin C, an amyloidogenic protein, dimerizes through three-dimensional domain swapping. *Nat Struct Biol* **2001**, *8*, 316-320.
- (28) Mares, J.; Stejskal, D.; Vavrouskova, J.; Urbanek, K.; Herzig, R. et al. Use of cystatin C determination in clinical diagnostics. *Biomed Pap Med Fac Univ Palacky Olomouc Czech Repub* **2003**, *147*, 177-180.
- (29) Jaskolski, M. 3D domain swapping, protein oligomerization, and amyloid formation. *Acta Biochim Pol* **2001**, *48*, 807-827.
- (30) Serpell, L. C.; Blake, C. C.; Fraser, P. E. Molecular structure of a fibrillar Alzheimer's A beta fragment. *Biochemistry* **2000**, *39*, 13269-13275.
- (31) Tycko, R. Insights into the amyloid folding problem from solid-state NMR. *Biochemistry* **2003**, *42*, 3151-3159.
- (32) Petkova, A. T.; Ishii, Y.; Balbach, J. J.; Antzutkin, O. N.; Leapman, R. D. et al. A

---

structural model for Alzheimer's beta -amyloid fibrils based on experimental constraints from solid state NMR. *Proc Natl Acad Sci U S A* **2002**, *99*, 16742-16747.

(33) Pike, C. J.; Walencewicz-Wasserman, A. J.; Kosmoski, J.; Cribbs, D. H.; Glabe, C. G. et al. Structure-activity analyses of beta-amyloid peptides: contributions of the beta 25-35 region to aggregation and neurotoxicity. *J Neurochem* **1995**, *64*, 253-265.

(34) Miravalle, L.; Tokuda, T.; Chiarle, R.; Giaccone, G.; Bugiani, O. et al. Substitutions at codon 22 of Alzheimer's abeta peptide induce diverse conformational changes and apoptotic effects in human cerebral endothelial cells. *J Biol Chem* **2000**, *275*, 27110-27116.

(35) Ghiso, J.; Frangione, B. Amyloidosis and Alzheimer's disease. *Adv Drug Deliv Rev* **2002**, *54*, 1539-1551.

(36) Esler, W. P.; Stimson, E. R.; Ghilardi, J. R.; Lu, Y. A.; Felix, A. M. et al. Point substitution in the central hydrophobic cluster of a human beta-amyloid congener disrupts peptide folding and abolishes plaque competence. *Biochemistry* **1996**, *35*, 13914-13921.

(37) Wahlbom, M.; Wang, X.; Lindstrom, V.; Carlemalm, E.; Jaskolski, M. et al. Fibrillogenic oligomers of human cystatin C are formed by propagated domain swapping. *J Biol Chem* **2007**, *282*, 18318-18326.

(38) Levy, E. Cystatin C: a potential target for Alzheimer's treatment. *Expert Rev Neurother* **2008**, *8*, 687-689.

(39) Dalboge, H.; Jensen, E. B.; Tottrup, H.; Grubb, A.; Abrahamson, M. et al. High-level expression of active human cystatin C in Escherichia coli. *Gene* **1989**, *79*, 325-332.

---

(40) Damoc, E.; Youhnovski, N.; Crettaz, D.; Tissot, J. D.; Przybylski, M. High resolution proteome analysis of cryoglobulins using Fourier transform-ion cyclotron resonance mass spectrometry. *Proteomics* **2003**, *3*, 1425-1433.

(41) Comeau, S. R.; Gatchell, D. W.; Vajda, S.; Camacho, C. J. ClusPro: a fully automated algorithm for protein-protein docking. *Nucleic Acids Res* **2004**, *32*, W96-99.

(42) Tovchigrechko, A.; Vakser, I. A. GRAMM-X public web server for protein-protein docking. *Nucleic Acids Res* **2006**, *34*, W310-314.

(43) Koradi, R.; Billeter, M.; Wuthrich, K. MOLMOL: a program for display and analysis of macromolecular structures. *J Mol Graph* **1996**, *14*, 51-55, 29-32.

## 6. APPENDIX

### 6.1 Appendix 1 – Abbreviations

<b>Abbreviations</b>	<b>Name</b>
<b>ACN</b>	Acetonitrile
<b>Ab</b>	Antibody
<b>APS</b>	Ammoniumperoxodisulfat
<b>CD</b>	Circular dichroism
<b>CDR</b>	Complementary determining region
<b>Da</b>	Dalton
<b>DHB</b>	Dihydroxybenzoic acid
<b>DTT</b>	Dithiothreitol
<b>EDC</b>	1-ethyl-3-(3-dimethylaminopropyl) carbodiimide
<b>ELISA</b>	Enzyme linked immunosorbent assay
<b>ESI-MS</b>	Electrospray/ionizations- Mass spectrometry
<b>HCCA</b>	4-Hydroxy- $\alpha$ -cyanamic acid
<b>HPLC</b>	High performance liquid chromatography
<b>MALDI-MS</b>	Matrix-assisted Laser desorptions-/ionizations-Mass Spectrometry
<b>min</b>	Minute
<b>m/z</b>	Mass over charge ratio
<b>NHS</b>	N-Hydroxysuccinimide
<b>PBS</b>	Phosphate buffered saline
<b>PD</b>	Parkinson disease
<b>pH</b>	Negative logarithmus of $H_3O^+$ -iones concentration
<b>SAM</b>	Self Assembled Monolayer
<b>SDS-PAGE</b>	Sodiumdodecylsulfat-Polyacrylamid-Gel electrophoresis
<b>TEMED</b>	N,N,N',N'-Tetramethylethyldiamine
<b>TFA</b>	Trifluoroacetic acid
<b>TOF</b>	Time of flight

<b>Tween</b>	Polyoxyethylen Sorbitan Monolaurat
<b>UV</b>	Ultraviolet
<b>°C</b>	Grad Celsius

## 6.2 Appendix 2 – Abbreviations for amino acids

*Table 5: Amino acids abbreviations.*

<b>Name</b>	<b>One letter code</b>	<b>Three letters code</b>	<b>Monoisotopic mass (Da)</b>
<b>Alanine</b>	A	Ala	71.03711
<b>Arginine</b>	R	Arg	156.10111
<b>Asparagine</b>	N	Asn	114.04293
<b>Aspartic Acid</b>	D	Asp	115.02694
<b>Cysteine</b>	C	Cys	103.00919
<b>Glutamine</b>	Q	Gln	123.05858
<b>Glutamic acid</b>	E	Glu	129.04259
<b>Glycine</b>	G	Gly	129.04259
<b>Histidine</b>	H	His	57.021046
<b>Isoleucine</b>	I	Ile	113.08406
<b>Leucine</b>	L	Leu	113.08406
<b>Lysine</b>	K	Lys	128.09496
<b>Methionine</b>	M	Met	131.04049
<b>Phenilalanine</b>	F	Phe	147.06841
<b>Proline</b>	P	Ro	97.05276
<b>Serine</b>	S	Ser	87.03203
<b>Threonine</b>	T	Thr	101.04768
<b>Tryptophan</b>	W	Trp	185.07931
<b>Tyrosine</b>	Y	Tyr	163.06333
<b>Valine</b>	V	Val	99.05841